

Minimax Regret Estimation for Generalizing Heterogeneous Treatment Effects with Multisite Data

Yi Zhang* Melody Huang[†] Kosuke Imai[‡]

Abstract

To test scientific theories and develop individualized treatment rules, researchers often wish to learn heterogeneous treatment effects that can be consistently found across diverse populations and contexts. We consider the problem of generalizing heterogeneous treatment effects (HTE) based on data from multiple sites. A key challenge is that a target population may differ from the source sites in unknown and unobservable ways. This means that the estimates from site-specific models lack external validity, and a simple pooled analysis risks bias. We develop a robust CATE (conditional average treatment effect) estimation methodology with multisite data from heterogeneous populations. We propose a minimax-regret framework that learns a generalizable CATE model by minimizing the worst-case regret over a class of target populations whose CATE can be represented as convex combinations of site-specific CATEs. Using robust optimization, the proposed methodology accounts for distribution shifts in both individual covariates and treatment effect heterogeneity across sites. We show that the resulting CATE model has an interpretable closed-form solution, expressed as a weighted average of site-specific CATE models. Thus, researchers can utilize a flexible CATE estimation method within each site and aggregate site-specific estimates to produce the final model. Through simulations and a real-world application, we show that the proposed methodology improves the robustness and generalizability of existing approaches.

Keywords: causal inference, conditional average treatment effect, distributional shift, external validity, generalizability, robust optimization, transportability

1 Introduction

A central objective of causal inference, shared by both scientific research and industry applications, is to uncover generalizable cause-and-effect relationships. Generalizing heterogeneous treatment effects (HTEs) is crucial in this pursuit, as identifying consistent HTEs across diverse populations can provide deeper insight into the underlying causal mechanisms. Estimating generalizable HTEs can also lead to more efficacious individualized treatment rules across heterogeneous populations, with applications ranging from precision medicine in the health sciences to data-driven decision-making in the social sciences.

*Ph.D. Student, Department of Statistics, Harvard University. 1 Oxford Street, Cambridge MA 02138. Email: yi_zhang@fas.harvard.edu

[†]Assistant Professor, Department of Political Science and Statistics & Data Science, Yale University. Email: melody.huang@yale.edu

[‡]Professor, Department of Government and Department of Statistics, Harvard University. 1737 Cambridge Street, Institute for Quantitative Social Science, Cambridge MA 02138. Email: imai@harvard.edu URL: <https://imai.fas.harvard.edu>

In this paper, we consider the problem of generalizing HTEs based on data from multiple sites. We consider robust estimation of the conditional average treatment effect (CATE) for a target population when it is possible to estimate the CATE specific to each source site. We address a common methodological challenge that the target population may differ from the source populations in unknown and unobservable ways. These differences can arise from observed and unobserved unit characteristics, the way in which treatment affects the outcome, and the details of what constitutes treatment (Egami and Hartman, 2023). In fact, treatment may not even have been administered in the target population. For example, a researcher can analyze multiple clinical trials to learn the CATE of a new drug for a general population.

In this challenging but commonly encountered setting, we develop a robust CATE estimation methodology based on multisite data from heterogeneous populations. Because target and source populations can differ in unknown ways, estimates from site-specific models lack external validity, whereas a naive pooled analysis also risks bias. We propose a *minimax-regret* framework to learn a generalizable CATE model by minimizing the worst-case regret relative to the oracle CATE model over a class of target populations (Section 2). Thus, the proposed approach guarantees robust predictive performance of individual treatment effects without specifying the exact relationship between the target and source site populations. To our knowledge, we are the first to consider the minimax regret criterion for robust CATE estimation with multisite data, although it has been explored for traditional statistical learning (e.g., Agarwal and Zhang, 2022; Mo et al., 2024) and policy learning (e.g., Lei et al., 2023).

Specifically, we consider a class of target populations whose CATE can be expressed as a convex combination of site-specific CATEs. We also assume that the marginal distribution of covariates in the target population is identifiable though the distribution can arbitrarily differ from that of any source site population. Under this broad class of target distributions, we derive a closed-form expression for the minimax-regret CATE model as a weighted average of site-specific CATE models. The aggregation weights are interpretable and can be computed directly from estimated site-specific CATE models without access to individual-level data in the source sites. Thus, our methods are communication efficient and privacy-preserving, while allowing the use of various machine learning models that have recently been developed to flexibly estimate the CATE from a single site (e.g., Hahn et al., 2020; Imai and Ratkovic, 2013; Künzel et al., 2019; Nie et al., 2021; Kennedy, 2023; Shalit et al., 2017; Wager and Athey, 2018).

Our theoretical analysis establishes the convergence rate of the proposed minimax regret CATE estimator, demonstrating that an accurate estimation of site-specific CATE leads to that of the minimax regret CATE. This requirement underscores the importance of using flexible machine learning methods for source sites. Finally, we compare the proposed minimax regret framework with two alternative approaches — the minimax risk approach, which minimizes the maximum risk, and the minimax relative-risk approach, which minimizes the risk relative to a baseline CATE model (Section 3). We show that, relative to the minimax regret CATE estimator, the minimax risk estimator tends to overfit to target distributions with higher noise levels, while the minimax relative-risk estimator is sensitive to the choice of the baseline CATE model. Through simulation studies and a real-world empirical application, we demonstrate the robust performance of the proposed methodology across a wide range of target distributions (Sections 4 and 5).

Related Literature

Estimation of HTEs with multisite data has gained significant attention in recent years (see Brantner et al., 2023, for a recent review). The most commonly used approaches are based on parametric models such as mixed-effects models (e.g., Debray et al., 2015; Burke et al., 2017; Seo et al., 2021).

Unfortunately, these methods are susceptible to bias caused by model misspecification. In contrast, the proposed minimax regret approach is nonparametric and places much weaker restrictions on cross-site treatment effect heterogeneity. Although some have recently developed nonparametric approaches based on machine learning (e.g., [Tan et al., 2022](#); [Shyr et al., 2023](#)), their focus is the estimation of site-specific CATEs. Instead, our framework aims to generalize CATE to a class of target populations by using data from multiple source sites.

Our work contributes to the growing literature on external validity (e.g., [Bareinboim and Pearl, 2016](#); [Curth et al., 2021](#); [Egami and Hartman, 2023](#); [Miratrix et al., 2021](#); [Stuart et al., 2015](#)). A common assumption in this literature is the transportability of the treatment effect model to a target population ([Kallus and Zhou, 2018](#); [Dahabreh and Hernán, 2019](#); [Dahabreh et al., 2023](#); [Yang et al., 2023](#); [Cheng and Cai, 2021](#); [Hatt et al., 2022](#); [Huang et al., 2023](#)). In practice, however, this assumption is often violated because of various observed and unobserved sources of cross-site heterogeneity. Some have developed sensitivity analyses that address this violation of assumption (e.g., [Huang, 2024a,b](#); [Nguyen et al., 2017](#); [Nie et al., 2021](#)), while others have proposed a sampling strategy to improve generalizability (e.g., [Egami and Lee, 2024](#); [Tipton and Mamakos, 2023](#)). These works, however, primarily focus on the average treatment effect (ATE), and none considers the robust estimation of CATE.

Our proposed robust optimization framework is also related to the growing literature on distributional robustness in causal inference. Much of this literature has focused on ATE estimation (e.g., [Jin et al., 2022](#); [Dorn et al., 2024](#); [Yadlowsky et al., 2018](#)) and policy learning (e.g., [Carranza and Athey, 2024](#); [Ishihara and Kitagawa, 2021](#); [Kallus and Zhou, 2021](#); [Kido, 2022](#); [Lei et al., 2023](#); [Manski, 2004](#); [Mo et al., 2021](#); [Stoye, 2012](#)). While [Kern et al. \(2024\)](#) studies CATE estimation, their framework is designed to be robust to unknown covariate shifts in the target distribution. In contrast, our approach addresses the additional challenge of unknown distributional shifts in treatment effect heterogeneity, leading to different methods.

Beyond causal inference, the minimax distributionally robust optimization (DRO) framework has been extensively studied in fields such as optimization ([Ben-Tal et al., 2013](#); [Duchi et al., 2021](#)), machine learning ([Duchi and Namkoong, 2021](#); [Sagawa et al., 2019](#)), and statistical learning theory ([Awasthi et al., 2023](#); [Zhang et al., 2023](#)). In the context of standard supervised learning, several minimax objectives have been proposed, including minimizing the worst-case risk ([Hu et al., 2018](#); [Sagawa et al., 2019](#)), the worst-case regret ([Mo et al., 2024](#); [Hastings et al., 2024](#); [Agarwal and Zhang, 2022](#)), and the worst-case explained variance or relative-risk ([Meinshausen and Bühlmann, 2015](#); [Wang et al., 2023](#)). For a detailed comparison of these minimax objectives, see [Mo et al. \(2024\)](#).

While [Mo et al. \(2024\)](#), [Wang et al. \(2023\)](#), and [Hastings et al. \(2024\)](#) also apply DRO to settings with multiple heterogeneous populations, they focus on traditional prediction problems with directly observed outcomes. These settings can leverage standard iterative optimization techniques to solve the minimax objective efficiently. In contrast, our work focuses on generalizing the CATE model across multiple heterogeneous source sites in the causal inference setting, where the outcomes are counterfactual and not directly observed. This distinction underscores the necessity and advantages of closed-form solutions in our framework, which require additional techniques to derive the final minimax CATE model. While our proposed minimax regret framework is closely related to that of [Mo et al. \(2024\)](#), their closed-form results are limited to linear regression models for prediction. In contrast, we consider a more general model class for CATE estimation, enabling the use of nonparametric machine learning models for flexible estimation.

2 Minimax Regret Distributionally Robust Learning

In this section, we introduce a minimax regret distributionally robust learning framework for generalizable CATE estimation. We begin by describing the problem setup, in which we have the data from multiple source sites but only observe covariates from a target population. We then propose the minimax regret CATE model, which minimizes the worst-case performance relative to the oracle CATE model over the range of plausible target populations, characterized as a convex combination of the source sites. We show that the closed-form solution is available under the proposed framework. This enables the separate and flexible estimation of CATE model within each source site. These estimated site-specific CATEs are then aggregated to produce the final minimax regret CATE model.

2.1 Setup

Suppose we have data from S source sites, indexed by $s \in [S] := \{1, \dots, S\}$. For each source site s , let $\mathbf{X}^{(s)} \in \mathcal{X}$ denote the pre-treatment covariates and $A^{(s)} \in \{0, 1\}$ denote the binary treatment indicator. We define $(Y^{(s)}(1), Y^{(s)}(0))$ as the potential outcomes under treatment $A^{(s)} = 1$ and control $A^{(s)} = 0$ conditions, respectively. For each unit $i = 1, \dots, n_s$ in source site s , we assume $(Y_i^{(s)}(1), Y_i^{(s)}(0), \mathbf{X}_i^{(s)})$ is drawn independently from a *site-specific* distribution $P^{(s)} = (P_{(Y(1), Y(0))|\mathbf{X}}^{(s)}, P_{\mathbf{X}}^{(s)})$, where $P_{(Y(1), Y(0))|\mathbf{X}=\mathbf{x}}^{(s)}$ is the conditional distribution of potential outcomes for the covariate value $\mathbf{x} \in \mathcal{X}$, and $P_{\mathbf{X}}^{(s)}$ represents the marginal covariate distribution. Under standard SUTVA assumptions (Rubin, 1990), the observed outcome variable is defined based on the realized treatment as $Y_i^{(s)} = A_i^{(s)} \cdot Y_i^{(s)}(1) + (1 - A_i^{(s)}) \cdot Y_i^{(s)}(0)$. Thus, for each source site s , we obtain n_s independent and identically distributed (i.i.d.) observations, denoted as $\left\{ Y_i^{(s)}, \mathbf{X}_i^{(s)}, A_i^{(s)} \right\}_{i=1}^{n_s}$.

For each source site s , we consider the *site-specific* conditional average treatment effect (CATE) function with respect to the distribution $P^{(s)}$, which is defined as,

$$\tau^{(s)}(\mathbf{x}) := \mathbb{E}_{P^{(s)}}[Y(1) - Y(0) \mid \mathbf{X} = \mathbf{x}] \quad (1)$$

for any given $\mathbf{x} \in \mathcal{X}$. Throughout the paper, we omit the superscript $^{(s)}$ for random variables when their respective distributions are clear from context. Given potential site-level differences, we allow $P^{(s)}$ to vary across sites, implying that distributional shifts may occur not only in covariates \mathbf{X} but also in the heterogeneous treatment effect, i.e., $Y(1) - Y(0)$ given \mathbf{X} . This means that we allow each source site to have a distinct, non-identical CATE function $\tau^{(s)}(\mathbf{x})$.

Our goal is to estimate a generalizable CATE model

$$\tau_Q(\mathbf{x}) := \mathbb{E}_Q[Y(1) - Y(0) \mid \mathbf{X} = \mathbf{x}]$$

with performance guarantees for a target population $Q = (Q_{(Y(1), Y(0))|\mathbf{X}}, Q_{\mathbf{X}})$. We consider the setting in which the marginal covariate distribution $Q_{\mathbf{X}}$ is identifiable for the target population, but its conditional distribution of potential outcomes given that the covariates $Q_{(Y(1), Y(0))|\mathbf{X}}$ may differ from those of source site populations in unknown ways. Specifically, we observe an i.i.d. sample of size n_Q from the target distribution where only pre-treatment covariates are observed for each unit, denoted by $\{\mathbf{X}_i^Q\}_{i=1}^{n_Q}$. This is a common scenario in practice, as researchers typically have access to pre-treatment covariates, even when treatment has not yet been administered.

2.2 Multisite Distributionally Robust Estimation Framework

We develop a methodology that leverages the availability of multiple source sites and achieves good overall prediction accuracy of heterogeneous treatment effects across a wide range of target populations. Specifically, we consider an *uncertainty set* of all plausible target distributions that are related to source site distributions. While the covariate distribution of this target population is assumed to be identifiable, we impose only a mild restriction on the unknown distribution of the heterogeneous treatment effect, $Y(1) - Y(0) \mid \mathbf{X}$. Specifically, we assume that the CATE function for the target population $\tau_Q(\cdot)$ can be expressed as a convex combination of the source site CATE functions, $\{\tau^{(s)}(\cdot)\}_{s=1}^S$. The formal definition of this multisite uncertainty set is given here.

Definition 1 (Multisite Uncertainty Set). Define the uncertainty set $\mathcal{C}(Q_{\mathbf{X}})$ as:

$$\mathcal{C}(Q_{\mathbf{X}}) := \left\{ Q = (Q_{\mathbf{X}}, Q_{(Y(1), Y(0)) \mid \mathbf{X}}) \mid \tau_Q(\cdot) = \sum_{s=1}^S q_s \cdot \tau^{(s)}(\cdot) \quad \text{with} \quad \mathbf{q} \in \Delta_{S-1} \right\} \quad (2)$$

where $\Delta_{S-1} = \left\{ \mathbf{q} \in \mathbb{R}^S \mid \sum_{s=1}^S q_s = 1, \min_s q_s \geq 0 \right\}$ denotes the $(S - 1)$ -dimensional simplex.

The uncertainty set restricts the class of joint distributions over $(Y(1), Y(0), \mathbf{X})$ to which the target population belongs. In particular, we formulate this constraint only on the CATE model $\tau_Q(\cdot)$ rather than directly restricting the entire conditional distribution of potential outcomes $Q_{(Y(1), Y(0)) \mid \mathbf{X}}$. Thus, our multisite uncertainty set spans the entire convex hull of the source CATE functions, ensuring that it is large enough to accommodate a wide range of discrepancies between the target and each source distribution, while avoiding being overly conservative.

We next develop a distributionally robust optimization (DRO) framework to learn a generalizable CATE model that is robust across all plausible target distributions in this multisite uncertainty set $\mathcal{C}(Q_{\mathbf{X}})$. We begin by observing that a CATE function, $\mathbb{E}[Y(1) - Y(0) \mid \mathbf{X} = \mathbf{x}]$, can be viewed as a *counterfactual* prediction model, where the outcome is the individual treatment effect $Y(1) - Y(0)$ and the predictors are the pre-treatment covariates \mathbf{X} . Our goal then is to derive a CATE model that achieves good prediction accuracy over the range of target populations given in Definition 1.

The standard approach in the DRO literature is to optimize the *worst-case* prediction performance over the uncertainty set. Formally, for a given model class \mathcal{F} and a general loss function $\ell : \mathbb{R} \times \mathbb{R} \rightarrow \mathbb{R}$, this minimax approach defines the robust prediction model as the solution to the following optimization problem:

$$f_{\text{risk}}^*(\cdot) := \arg \min_{f \in \mathcal{F}} \max_{Q \in \mathcal{C}(Q_{\mathbf{X}})} \mathbb{E}_Q[\ell(Y(1) - Y(0), f(\mathbf{X}))], \quad (3)$$

where $f_{\text{risk}}^*(\cdot)$ minimizes the *worst-case prediction risk* over the uncertainty set $\mathcal{C}(Q_{\mathbf{X}})$. While the minimax approach based on the raw risk objective is conceptually straightforward and has been widely studied in the DRO literature (see, e.g., Ben-Tal et al., 2013; Duchi and Namkoong, 2021; Zhang et al., 2023), its solutions are often overly pessimistic because the objective is highly sensitive to varying noise levels across target distributions in the uncertainty set (e.g., Agarwal and Zhang, 2022; Hastings et al., 2024); see also Section 3.1.

Thus, we propose an alternative *minimax regret* objective (Savage, 1951; Manski, 2011). We define the *regret* (or *excess risk*) of a prediction model $f(\cdot)$ as the difference in risk between $f(\cdot)$ and the oracle optimal model in the model class \mathcal{F} for a given target distribution Q :

$$\mathbb{E}_Q[(Y(1) - Y(0) - f(\mathbf{X}))^2] - \min_{f' \in \mathcal{F}} \mathbb{E}_Q[(Y(1) - Y(0) - f'(\mathbf{X}))^2]. \quad (4)$$

Throughout the paper, we focus on the standard regression setting with continuous outcomes and, therefore, use the squared error loss in our definitions. While our proposed methodology can be applied to binary outcomes, we do not study classification loss functions (e.g., 0-1 loss or entropy loss) and leave extensions to classification settings for future work.

The proposed minimax regret CATE model minimizes the worst-case regret across the range of target distributions in $\mathcal{C}(Q_{\mathbf{X}})$:

$$f_{\text{regret}}^*(\cdot) = \arg \min_{f \in \mathcal{F}} \max_{Q \in \mathcal{C}(Q_{\mathbf{X}})} \left\{ \mathbb{E}_Q[(Y(1) - Y(0) - f(\mathbf{X}))^2] - \min_{f' \in \mathcal{F}} \mathbb{E}_Q[(Y(1) - Y(0) - f'(\mathbf{X}))^2] \right\}. \quad (5)$$

Unlike minimax risk CATE, this minimax regret CATE model minimizes the worst-case performance gap relative to the best possible model that achieves the best prediction of individual treatment effect for every choice of the target population Q . This accounts for differences in inherent learning difficulties across distributions, preventing a small number of challenging target populations from dominating the final solution and making the resulting model more robust to heterogeneous noise levels across distributions.

2.3 Closed-form Identification Result

Solving the DRO problem in Equation (5) is challenging for two reasons. First, the individual treatment effect $Y(1) - Y(0)$ is a counterfactual quantity and is not directly observable. Second, the target distribution Q is unknown and may differ from the observed source-site distributions, $\{P^{(s)}\}_{s \in [S]}$. To address these challenges, we derive a closed-form solution to this optimization problem under the assumption that the model class \mathcal{F} is large enough to contain the convex hull of CATE models from the source sites, $\{\tau^{(s)}(\cdot)\}_{s \in [S]}$. This assumption is likely to hold due to the availability of powerful machine learning methods for nonparametric CATE estimation in single-source settings, ensuring that the best possible CATE model within the class can accurately represent the oracle CATE model for each target population.

Consequently, we can reformulate the original optimization problem in Equation (5) as:

$$f_{\text{regret}}^*(\cdot) = \arg \min_{f \in \mathcal{F}} \max_{Q \in \mathcal{C}(Q_{\mathbf{X}})} \mathbb{E}_{Q_{\mathbf{X}}}[(f(\mathbf{X}) - \tau_Q(\mathbf{X}))^2]. \quad (6)$$

This reformulation reveals that the proposed robust CATE directly minimizes the worst-case mean squared error (MSE) of estimating the true CATE model τ_Q with respect to the fixed covariate distribution $Q_{\mathbf{X}}$. While this type of MSE objective is widely used as an evaluation criterion in the CATE estimation literature (Künzel et al., 2019; Curth and Van der Schaar, 2021), we directly embed it as a minimax learning objective in the optimization framework.

We will begin by first showing that the problem in Equation (6), in which we optimize over an infinite set of distributions within the convex hull, is equivalent to solving a constrained optimization problem, with a finite number of constraints corresponding to the vertices of the convex hull. This intermediate result provides an important intuition about our key identification theorem.

Proposition 1 (Alternative representation of the minimax regret problem). The minimax problem defined in Equation (6) can be equivalently expressed as:

$$\{f_{\text{regret}}^*(\cdot), R^*\} = \arg \min_{f \in \mathcal{F}, R \in \mathbb{R}} R \quad \text{subject to} \quad \mathbb{E}_{Q_{\mathbf{X}}}[(f(\mathbf{X}) - \tau^{(s)}(\mathbf{X}))^2] \leq R \quad \text{for all } s \in [S], \quad (7)$$

where R^* denotes the smallest worst-case regret achieved by $f_{\text{regret}}^*(\cdot)$. Furthermore, the solution $\{f_{\text{regret}}^*(\cdot), R^*\}$ exists and satisfies the following conditions:

$$\begin{aligned}
f_{\text{regret}}^*(\cdot) &= \sum_{s=1}^S q_s^* \cdot \tau^{(s)}(\cdot) \quad \text{subject to} \quad q_s^* \cdot \left(\mathbb{E}_{Q_{\mathbf{X}}} [(f_{\text{regret}}^*(\mathbf{X}) - \tau^{(s)}(\mathbf{X}))^2] - R^* \right) = 0 \quad \text{for } s \in [S], \\
&\mathbb{E}_{Q_{\mathbf{X}}} [(f_{\text{regret}}^*(\mathbf{X}) - \tau^{(s)}(\mathbf{X}))^2] \leq R^* \quad \text{for } s \in [S], \\
&\sum_{s=1}^S q_s^* = 1, \quad q_s^* \geq 0 \quad \text{for } s \in [S].
\end{aligned} \tag{8}$$

The proof is provided in Appendix C.1. Proposition 1 implies that the minimax CATE $f_{\text{regret}}^*(\cdot)$ will be a convex combination of the CATEs from the source sites. Specifically, a source site s does not contribute to the final solution (i.e., $q_s^* = 0$) if the squared L_2 -distance between its CATE and $f_{\text{regret}}^*(\cdot)$ is strictly less than R^* . In contrast, a source site with a nonzero weight ($q_s^* > 0$) has a CATE exactly at the squared L_2 -distance of R^* from $f_{\text{regret}}^*(\cdot)$. Thus, these source sites define the minimax regret boundary.

To further motivate the minimax regret solution and its relationship with the CATE functions of the source sites, we present a simple example. Assume that site-specific CATE models are piecewise linear with an interaction term, $\tau^{(s)}(\mathbf{X}) = \beta_s \cdot X_1 \mathbb{1}(X_1 > 0) + X_1 X_2$, where $\beta_s \in \mathbb{R}$ controls cross-site heterogeneity. Then, in this setting, the resulting minimax regret CATE model is given by $f_{\text{regret}}^*(\cdot) = \beta_{\text{regret}}^* \cdot X_1 \mathbb{1}(X_1 > 0) + X_1 X_2$, which retains the same functional form as the source CATEs. Specifically, the minimax coefficient β_{regret}^* is derived from the optimization problem as $\beta_{\text{regret}}^* = \arg \min_{\beta \in \mathbb{R}} \max_{s \in [S]} (\beta - \beta_s)^2 = \frac{1}{2} (\max_{s \in [S]} \beta_s + \min_{s \in [S]} \beta_s)$. In other words, the minimax regret solution corresponds to the midpoint between the CATE models associated with the two boundary groups that have the highest and lowest values of β_s . This midpoint selection minimizes the worst-case MSE across source sites by balancing the maximum deviation from both extremes in the convex hull of site-specific CATEs.

Using Proposition 1, we now establish our main identification result for the oracle minimax regret CATE, showing that it can be represented as a weighted combination of the site-specific CATE models.

Theorem 1 (Minimax regret identification). Define $L_2(Q_{\mathbf{X}})$ as the space of square-integrable measurable functions with respect to $Q_{\mathbf{X}}$. Suppose that the model class $\mathcal{F} \subset L_2(Q_{\mathbf{X}})$ is convex and contains all the site-specific CATEs, i.e., $\tau^{(s)}(\cdot) \in \mathcal{F}$ for all $s \in [S]$. Then, the oracle minimax regret CATE $f_{\text{regret}}^*(\cdot)$ defined in Equation (5) can be identified as:

$$f_{\text{regret}}^*(\cdot) = \sum_{s=1}^S q_s^* \cdot \tau^{(s)}(\cdot) \quad \text{with} \quad \mathbf{q}^* = \arg \min_{\mathbf{q} \in \Delta_{S-1}} \mathbf{q}^\top \Gamma \mathbf{q} - \mathbf{q}^\top \mathbf{d}, \tag{9}$$

where the (k, l) -th element of $S \times S$ matrix Γ is given by $\Gamma_{k,l} = \mathbb{E}_{Q_{\mathbf{X}}} [\tau^{(k)}(\mathbf{X})\tau^{(l)}(\mathbf{X})]$ for $k, l \in [S]$, and $\mathbf{d} := (\Gamma_{1,1}, \dots, \Gamma_{S,S})^\top$ is the diagonal vector of Γ .

The proof is given in Appendix C.2. The aggregation weights $\mathbf{q}^* = \{q_s^*\}_{s=1}^S$ determine the contribution of each source site to the final CATE model. These weights are found by solving the quadratic optimization problem given in Equation (9), where Γ is, by construction, a symmetric and positive semidefinite matrix. The objective function for determining the aggregation weights comprises two main components. The first is a quadratic term, $\mathbf{q}^\top \Gamma \mathbf{q} = \mathbb{E}_{Q_{\mathbf{X}}} \left[\left(\sum_{s=1}^S q_s \cdot \tau^{(s)}(\mathbf{X}) \right)^2 \right]$,

representing the L_2 -distance of the aggregated model from the origin. The second is a linear term, $\mathbf{q}^\top \mathbf{d} = \mathbb{E}_{Q_{\mathbf{X}}} \left[\sum_{s=1}^S q_s \cdot \tau^{(s)}(\mathbf{X})^2 \right]$, denoting the weighted average of the second moments of each site-specific CATE, both measured with respect to the target covariate distribution $Q_{\mathbf{X}}$. This result implies that if the source-site CATE functions are known, we can directly compute the aggregation weights and construct $f_{\text{regret}}^*(\cdot)$ using Equation (9). This computational efficiency is a major advantage of the proposed methodology over many other existing minimax methods.

In particular, the resulting solution is agnostic to the specification of the model class, enabling a wide range of flexible single-site CATE estimation methods proposed in the literature. To our knowledge, we are the first to derive a closed-form solution to the minimax regret optimization problem under a flexible model class \mathcal{F} . While Mo et al. (2024) also obtains a closed-form expression in a similar multisite setup, the result is limited to linear regression in the standard supervised learning setting. In contrast, our result is based on a considerably larger model class, enabling the use of many popular nonparametric estimators and machine learning models to approximate complex CATE functions. Our framework does not require site-specific CATEs to share the same functional form, assuming only that the model class \mathcal{F} encompasses all site-specific CATEs $\{\tau^{(s)}(\cdot)\}_{s=1}^S$. In practice, one can estimate these site-specific CATEs separately using different methods before aggregating the resulting CATE models (see Section 2.5 for more details).

2.4 Identification with Additional Restrictions

If site-specific CATE models are highly heterogeneous, optimizing worst-case performance over the entire uncertainty set may yield an overly conservative solution. In such cases, additional restrictions on the target population, assuming that they can be justified, lead to more informative inference. We generalize the proposed methodology so that researchers can incorporate auxiliary information on the target distribution by further restricting the uncertainty set. Specifically, we assume that the combination weights lie within a convex subset of the simplex, $\mathcal{H} \subseteq \Delta_{S-1}$:

$$\mathcal{C}(Q_{\mathbf{X}}, \mathcal{H}) := \left\{ Q = (Q_{\mathbf{X}}, Q_{(Y(1), Y(0))|\mathbf{X}}) \mid \tau_Q(\cdot) = \sum_{s=1}^S q_s \cdot \tau^{(s)}(\cdot) \quad \text{with} \quad \mathbf{q} \in \mathcal{H} \right\}, \quad (10)$$

where the constraint set \mathcal{H} is chosen by researchers. For example, one may impose the maximal value of site-specific weights to limit the influence of any single source site on the final CATE model, i.e., $q_s \leq c$ for all $s \in [S]$ where $c \in (1/S, 1)$.

Given the generalized uncertainty set $\mathcal{C}(Q_{\mathbf{X}}, \mathcal{H})$, we can define the minimax regret CATE model over $\mathcal{C}(Q_{\mathbf{X}}, \mathcal{H})$ as in Equation (6), denoting it by $f_{\text{regret}, \mathcal{H}}^*(\cdot)$. We extend Theorem 1 by deriving a closed-form solution under the assumption that \mathcal{H} is a convex polytope within the simplex Δ_{S-1} . To derive this result, we leverage the fact that any polytope can be represented as the convex hull of a finite set of points.

Corollary 1 (Extension to polytopes $\mathcal{H} \subset \Delta_{S-1}$). Let \mathcal{H} be a convex polytope within the $(S-1)$ dimensional simplex Δ_{S-1} , represented as the convex hull of a finite set of vertices $\{\mathbf{g}_1, \dots, \mathbf{g}_N\}$, where each vertex \mathbf{g}_i is a distinct element of the simplex, i.e., $\mathbf{g}_i \in \Delta_{S-1} \subset \mathbb{R}^S$ for $i \in [N]$. Define the transformation matrix $G = (\mathbf{g}_1, \dots, \mathbf{g}_N) \in \mathbb{R}^{S \times N}$. Under the same conditions as in Theorem 1, $f_{\text{regret}, \mathcal{H}}^*(\cdot)$ can be identified as:

$$f_{\text{regret}, \mathcal{H}}^*(\cdot) = (\mathbf{q}^*)^\top \boldsymbol{\tau}_{\text{poly}}(\cdot) \quad \text{with} \quad \mathbf{q}^* = \arg \min_{\mathbf{q} \in \Delta_{N-1}} \left(\mathbf{q}^\top \Gamma_{\text{poly}} \mathbf{q} - \mathbf{q}^\top \mathbf{d}_{\text{poly}} \right), \quad (11)$$

where $\boldsymbol{\tau}_{\text{poly}}(\cdot) = G^\top \boldsymbol{\tau}(\cdot)$, with $\boldsymbol{\tau}(\cdot) := (\tau^{(1)}(\cdot), \dots, \tau^{(S)}(\cdot))^\top$ representing the vector of site-specific CATE models, $\Gamma_{\text{poly}} = G^\top \Gamma G$, and

$$\mathbf{d}_{\text{poly}} := \left(\mathbb{E}_{Q_{\mathbf{X}}} \left[\left(\mathbf{g}_1^\top \boldsymbol{\tau}(\mathbf{X}) \right)^2 \right], \dots, \mathbb{E}_{Q_{\mathbf{X}}} \left[\left(\mathbf{g}_N^\top \boldsymbol{\tau}(\mathbf{X}) \right)^2 \right] \right)^\top$$

representing the diagonal vector of Γ_{poly} .

The proof is given in Appendix C.3. For notational simplicity, we focus on using $\mathcal{C}(Q_{\mathbf{X}})$ in the remainder of the paper, unless otherwise stated. The proposed estimation method and theoretical results extend naturally to a general uncertainty set $\mathcal{C}(Q_{\mathbf{X}}, \mathcal{H})$ introduced here.

2.5 Flexible Two-step Estimation Procedure

Given the identification result in Theorem 1, we can directly estimate the minimax CATE model $f_{\text{regret}}^*(\cdot)$ using the observed data. The estimation procedure consists of two steps: (1) estimate each site-specific CATE model, $\tau^{(s)}(\cdot)$ for $s = 1, \dots, S$; and (2) solve for the optimal aggregation weights \mathbf{q}^* , then obtain the final robust CATE model as an ensemble of the site-specific CATE models.

The key advantage of our robust CATE estimator is that it allows the use of any available machine learning algorithm to estimate site-specific CATEs (see, e.g., Hahn et al., 2020; Imai and Ratkovic, 2013; Kennedy, 2023; Künzel et al., 2019; Nie and Wager, 2021; Wager and Athey, 2018). Each source-site CATE can be estimated independently, potentially using different methods across sites. In addition, unlike other distributed learning methods, our two-step estimation procedure avoids the need to share individual-level data across sites (Sagawa et al., 2019; Hu et al., 2018) or employ iterative optimization (Deng et al., 2020; Mo et al., 2024). Therefore, our approach is both communication efficient and privacy-preserving.

Formally, to estimate $\tau^{(s)}(\cdot)$ using observed data, we impose the standard assumptions of unconfoundedness and positivity in the CATE estimation literature.

Assumption 1 (Identifiability within a source site). For each site $s \in [S]$, we assume that

- (a) *Unconfoundedness*: $Y_i^{(s)}(a) \perp\!\!\!\perp A_i^{(s)} \mid \mathbf{X}_i^{(s)} = \mathbf{x}$
- (b) *Positivity*: $\exists \epsilon > 0$ such that $\epsilon < \mathbb{P}(A_i^{(s)} = a \mid \mathbf{X}_i^{(s)} = \mathbf{x}) < 1 - \epsilon$, for $a \in \{0, 1\}$

Assumption 1 ensures that within each site, the CATE model $\tau^{(s)}(\cdot)$ is identifiable and can be consistently estimated using its locally observed data alone.

To ensure that the final robust CATE model performs well on the target covariate distribution $Q_{\mathbf{X}}$, we assume that $Q_{\mathbf{X}}$ lies within the support of each site-specific covariate distribution, $P_{\mathbf{X}}^{(s)}$ for $s \in [S]$. The assumption allows us to aggregate site-specific CATE models, each of which is estimated using local observed data, while avoiding extrapolation.

Assumption 2 (Covariate overlap). For each source site $s \in [S]$, we assume that the target covariate distribution $Q_{\mathbf{X}}$ is absolutely continuous with respect to $P_{\mathbf{X}}^{(s)}$, i.e., $\sup_{\mathbf{x} \in \mathcal{X}} dQ_{\mathbf{X}}(\mathbf{x})/dP_{\mathbf{X}}^{(s)}(\mathbf{x}) < \infty$.

Under Assumptions 1 and 2, we can construct the plug-in estimator of $f_{\text{regret}}^*(\cdot)$ based on Theorem 1:

$$\hat{f}_{\text{regret}}(\cdot) = \sum_{s=1}^S \hat{q}_s \cdot \hat{\tau}^{(s)}(\cdot) \quad \text{with} \quad \hat{\mathbf{q}} = \arg \min_{\mathbf{q} \in \Delta_{S-1}} \mathbf{q}^\top \hat{\Gamma} \mathbf{q} - \mathbf{q}^\top \hat{\mathbf{d}}, \quad (12)$$

where each entry of $\hat{\Gamma}$ and $\hat{\mathbf{d}}$ is estimated using empirical observations from the target population, $\{\mathbf{X}_i^Q\}_{i=1}^{n_Q}$, given by

$$\hat{\Gamma}_{k,l} = \frac{1}{n_Q} \sum_{i=1}^{n_Q} \hat{\tau}^{(k)}(\mathbf{X}_i^Q) \hat{\tau}^{(l)}(\mathbf{X}_i^Q) \quad \text{for } k, l \in [S],$$

$$\hat{d}_s = \frac{1}{n_Q} \sum_{i=1}^{n_Q} \left(\hat{\tau}^{(s)}(\mathbf{X}_i^Q) \right)^2 \quad \text{for } s \in [S].$$

We use $\hat{\tau}^{(s)}(\cdot)$ to denote a generic estimator of $\tau^{(s)}(\cdot)$ for each $s \in [S]$.

2.6 Theoretical Results

We establish the theoretical guarantees for the proposed minimax regret CATE estimator $\hat{f}_{\text{regret}}(\cdot)$ introduced in Section 2.5. Specifically, we derive the rate of convergence towards the true minimax regret CATE model $f_{\text{regret}}^*(\cdot)$.

We first introduce several necessary assumptions.

Assumption 3 (Positive definiteness). The number of source sites S is fixed and finite. The matrix Γ defined in Theorem 1 is positive definite with its smallest eigenvalue $\lambda_{\min}(\Gamma) > 0$.

While Γ is a positive semi-definite matrix by definition, we further assume that it is positive definite. This ensures that the objective function to determine the optimal aggregation weights in Theorem 1 is strictly convex, guaranteeing a unique solution \mathbf{q}^* . In practice, this assumption is easily satisfied as long as the site-specific CATE models $\{\tau^{(s)}(\cdot)\}_{s=1}^S$ are linearly independent.

In addition, we assume that the outcome is bounded and that the site-specific CATE estimators are L_2 consistent with respect to the target covariate distribution. Specifically, for a function $f(\cdot)$, we define its L_q norm measured over the target covariate distribution $Q_{\mathbf{X}}$ as $\|f(\cdot)\|_{Q,q} := (\mathbb{E}_{Q_{\mathbf{X}}} [f(\mathbf{X})^q])^{1/q}$ where $q \geq 1$.

Assumption 4 (Bounded outcome). We assume that the potential outcomes $Y_i(a)$ are almost surely bounded, i.e., $\exists M \geq 0$ such that $|Y_i(a)| \leq M$.

Assumption 5 (L_2 consistent estimation of site-specific CATE models). Let $n = \min_{s \in [S]} n_s$ denote the smallest sample size among the S source sites. We assume that there exists a positive sequence δ_n converging to zero as n grows such that

$$\max_{s \in [S]} \left\| \hat{\tau}^{(s)}(\cdot) - \tau^{(s)}(\cdot) \right\|_{Q,2} \leq \delta_n.$$

Assumption 5 constrains the L_2 convergence rate of $\hat{\tau}^{(s)}(\cdot)$ over the target covariate distribution. In the current literature, the convergence rates have been established for different CATE estimators under various conditions (see Appendix B).

The following theorem establishes the convergence rate for the proposed minimax regret CATE estimator $\hat{f}_{\text{regret}}(\cdot)$ defined in Equation (12).

Theorem 2 (L_2 error for the minimax regret CATE estimator). Suppose that Assumptions 1–5 hold. Then, with probability greater than $1 - \frac{1}{t} - \frac{1}{t^2}$ for $t > 1$,

$$\left\| \hat{f}_{\text{regret}}(\cdot) - f_{\text{regret}}^*(\cdot) \right\|_{Q,2} \leq \sqrt{2S} \left[\delta_n + 2M \left\{ \frac{1.5tS^2}{\lambda_{\min}(\Gamma)} \left(\frac{4M}{\sqrt{tS}} \delta_n + \delta_n^2 + \frac{4M^2}{\sqrt{n_Q}} \right) \wedge \rho_{\Delta_{S-1}} \right\} \right],$$

where $\rho_{\Delta_{S-1}} := \max_{\mathbf{q}, \mathbf{q}' \in \Delta_{S-1}} \|\mathbf{q} - \mathbf{q}'\|_2$ is the constant diameter of the simplex Δ_{S-1} .

The proof is given in Appendix C.4. Theorem 2 characterizes the estimation error of $\hat{f}_{\text{regret}}(\cdot)$ with two main components. The first term, δ_n , originates from the direct estimation error of site-specific CATE models, while the second term, which depends on $\frac{1}{\lambda_{\min}(\Gamma)} \left(\delta_n + \delta_n^2 + \frac{1}{\sqrt{n_Q}} \right)$, originates from the estimation error of the aggregated weights $\{\hat{q}_s\}_{s \in [S]}$. In particular, both the (smallest) sample size of the source site data, n , and the sample size of the target covariate data, n_Q , affect the accuracy of $\hat{f}_{\text{regret}}(\cdot)$. As δ_n and $\frac{1}{\sqrt{n_Q}}$ approach zero, this error bound shrinks, eventually falling below the naive constant upper bound $\rho_{\Delta_{S-1}}$. Therefore, accurately recovering the oracle robust CATE model requires that each site-specific CATE model be estimated with reasonable precision. Additionally, the linear dependence among site-specific CATE models influences the error bound through the smallest eigenvalue $\lambda_{\min}(\Gamma)$ of the correlation matrix Γ . As $\lambda_{\min}(\Gamma) \rightarrow 0$, which indicates near-linear dependence of site-specific CATE models $\{\tau^{(s)}\}_{s \in [S]}$, estimating the optimal aggregation weights becomes more challenging.

Using Theorem 2, we can quantify the MSE between the estimator $\hat{f}_{\text{regret}}(\cdot)$ and a given target CATE model $\tau_Q(\cdot)$. Suppose that there is a fixed target distribution with covariate distribution $Q_{\mathbf{X}}$ and a true CATE model $\tau_Q(\cdot)$. Then, the MSE between $\hat{f}_{\text{regret}}(\cdot)$ and $\tau_Q(\cdot)$ can be bounded by:

$$\begin{aligned} \left\| \hat{f}_{\text{regret}} - \tau_Q \right\|_{Q,2}^2 &\leq \left\| \hat{f}_{\text{regret}} - f_{\text{regret}}^* \right\|_{Q,2}^2 + \left\| \tau_Q - f_{\text{regret}}^* \right\|_{Q,2}^2 \\ &\quad + 2 \left\| \hat{f}_{\text{regret}} - f_{\text{regret}}^* \right\|_{Q,2} \left\| \tau_Q - f_{\text{regret}}^* \right\|_{Q,2}. \end{aligned}$$

Therefore, the performance of the robust CATE estimator $\hat{f}_{\text{regret}}(\cdot)$ on any fixed target distribution Q depends on two factors: the convergence rate of $\hat{f}_{\text{regret}}(\cdot)$ to its population counterpart, and the inherent distance between the oracle CATE models $\tau_Q(\cdot)$ and $f_{\text{regret}}^*(\cdot)$. Specifically, when the sample sizes for both the source sites and the target covariate distribution are sufficiently large, the L_2 error for the minimax regret estimator, $\left\| \hat{f}_{\text{regret}} - f_{\text{regret}}^* \right\|_{Q,2}$, will shrink to zero. As a result, the distance between the minimax regret CATE estimator and any target CATE will converge to their true oracle gap, $\left\| \tau_Q - f_{\text{regret}}^* \right\|_{Q,2}$. However, as the uncertainty set of target distributions becomes larger, the worst-case MSE between the robust CATE estimator and target CATEs increases, indicating that it becomes more challenging to build a generalizable CATE model that performs consistently well across a wide range of heterogeneous distributions.

3 Comparison with Other Minimax Approaches

In this section, we investigate the properties of the robust CATE models derived from two alternative objectives — minimax risk and minimax relative risk —, and compare their properties with those of the proposed minimax regret CATE model. Although many of these existing works consider standard supervised learning problems (Mo et al., 2024; Wang et al., 2023; Hastings et al., 2024), we keep our discussion focused on the CATE estimation in causal inference.

3.1 Minimax Risk

As briefly mentioned in Section 2.2, a common approach in the multi-group DRO framework is to minimize the maximum risk rather than the regret (Duchi and Namkoong, 2021; Zhang et al., 2023). For comparison, we consider the robust CATE estimator based on the following minimax

squared-error objective:

$$f_{\text{risk}}^* = \arg \min_{f \in \mathcal{F}} \max_{Q \in \mathcal{C}(Q_{\mathbf{X}})} \mathbb{E}_Q[(Y(1) - Y(0) - f(\mathbf{X}))^2]. \quad (13)$$

A main problem of this formulation is that the resulting minimax risk CATE estimator can be sensitive to different noise levels across source sites. To illustrate this, we decompose the objective function using the law of total expectation as follows:

$$\mathbb{E}_Q[(\tau_Q(\mathbf{X}) - f(\mathbf{X}))^2] + \mathbb{E}_Q[\text{Var}_Q(Y(1) - Y(0) \mid \mathbf{X})]. \quad (14)$$

Compared to the minimax regret problem shown in Equation (6), the minimax risk problem includes an additional conditional variance term, which represents the noise level in the individual treatment effect conditional on covariates for the target distribution Q . By optimizing this objective, the minimax risk solution will adapt to differences in inherent learning difficulty across populations. When noise levels vary across target distributions, this minimax risk problem may lead to overfitting to those high-variance distributions that are heavily influenced by a few noisy sites.

In addition, the conditional variance in Equation (14) is generally unidentifiable since we never observe $Y(1)$ and $Y(0)$ at the same time. This makes it difficult to obtain an identifiable closed-form solution using the minimax risk estimation approach. In Appendix A, however, we derive a closed-form expression for the minimax risk estimator in the special case of $S = 2$ with a more restrictive uncertainty set. The result further illustrates the sensitivity of the minimax estimator to a target population with a high variance.

3.2 Minimax Relative-risk

Another minimax objective is based on a relative-risk function, which compares the prediction accuracy of a model $f(\cdot)$ against a pre-specified baseline model $f_{\text{base}}(\cdot)$. We can then define the minimax relative-risk CATE estimator as:

$$f_{\text{rel}}^*(\cdot; f_{\text{base}}) = \arg \min_{f \in \mathcal{F}} \max_{Q \in \mathcal{C}(Q_{\mathbf{X}})} \mathbb{E}_Q [(Y(1) - Y(0) - f(\mathbf{X}))^2 - (Y(1) - Y(0) - f_{\text{base}}(\mathbf{X}))^2]. \quad (15)$$

This type of objective, which benchmarks a decision rule against a natural baseline, has been used for robust optimization in policy learning (Ben-Michael et al., 2021; Kallus and Zhou, 2021; Lei et al., 2023) and supervised learning (Meinshausen and Bühlmann, 2015; Wang et al., 2023).

When \mathcal{F} contains the convex hull of true site-specific CATEs, the above objective function is equivalent to the L_2 -distance between the model $f(\cdot)$ and the true CATE, normalized by the distance between the baseline model and the true CATE:

$$\mathbb{E}_Q[(\tau_Q(\mathbf{X}) - f(\mathbf{X}))^2] - \mathbb{E}_Q[(\tau_Q(\mathbf{X}) - f_{\text{base}}(\mathbf{X}))^2]. \quad (16)$$

This objective provides a robustness guarantee by ensuring that $f_{\text{rel}}^*(\cdot)$ performs at least as well as $f_{\text{base}}(\cdot)$. Unlike the minimax regret objective, which compares a prediction model $f(\cdot)$ to the optimal CATE model within each target distribution Q , the relative-risk approach benchmarks $f(\cdot)$ against a common baseline model. As a result, the properties of $f_{\text{rel}}^*(\cdot)$ depend heavily on the choice of the baseline model.

In practice, selecting an appropriate baseline model often requires additional prior information. A common default choice is the zero constant model $f_{\text{base}} = 0$, which was originally proposed by Meinshausen and Bühlmann (2015) in classical linear regression settings (see also Guo, 2023) and later adopted by Wang et al. (2023) for statistical machine learning. When $f_{\text{base}} = 0$ and assuming

that the treatment effect is centered, i.e., the ATE $\mathbb{E}_{P^{(s)}}[Y(1) - Y(0)] = 0$ for $s = 1, \dots, S$, the negative value of the objective in Equation (15) can be interpreted as the variance explained by the model f . Thus, the solution f_{rel}^* ensures improved performance over the zero null model when predicting individual treatment effects. In the statistical learning literature, this objective is often referred to as the *maximin explained variance* (Guo, 2023; Wang et al., 2023).

Here, we derive a closed-form solution for the minimax relative-risk estimator f_{rel}^* for any baseline model f_{base} . In particular, due to the convex-concave structure of the optimization problem in Equation (15), this closed-form solution holds for the generalized uncertainty set $\mathcal{C}(Q_{\mathbf{X}}, \mathcal{H})$ over any convex subset $\mathcal{H} \subseteq \Delta_{S-1}$.

Proposition 2 (Minimax relative-risk identification). Suppose that the function class \mathcal{F} is convex with $\tau^{(s)}(\cdot) \in \mathcal{F}$ for all $s \in [S]$ and \mathcal{H} is a convex subset of Δ_{S-1} . Then $f_{\text{rel}}^*(\cdot; f_{\text{base}})$ in Equation (15), when optimized over $\mathcal{C}(Q_{\mathbf{X}}, \mathcal{H})$, can be identified as

$$f_{\text{rel}}^*(\cdot; f_{\text{base}}) = \sum_{s=1}^S q_s^* \cdot \tau^{(s)}(\cdot) \quad \text{with} \quad \mathbf{q}^* = \arg \min_{\mathbf{q} \in \mathcal{H}} \mathbb{E}_{Q_{\mathbf{X}}} \left[\sum_{s=1}^S q_s \cdot \tau^{(s)}(\mathbf{X}) - f_{\text{base}}(\mathbf{X}) \right]^2. \quad (17)$$

The proof is given in Appendix C.5. According to this proposition, the minimax relative-risk CATE estimator $f_{\text{rel}}^*(\cdot; f_{\text{base}})$ can be expressed as a weighted combination of site-specific CATE models $\{\tau^{(s)}(\cdot)\}_{s=1}^S$. This is similar to the minimax regret estimator in Theorem 1. The aggregation weights, however, are determined by minimizing the distance between the aggregated model and the baseline model. Thus, the performance of f_{rel}^* depends critically on a reasonable f_{base} . In particular, if $f_{\text{base}}(\cdot)$ lies within the uncertainty set $\mathcal{C}(Q_{\mathbf{X}}, \mathcal{H})$, the minimax relative-risk CATE estimator $f_{\text{rel}}^*(\cdot; f_{\text{base}})$ will simply reduce to $f_{\text{base}}(\cdot)$. If $f_{\text{base}}(\cdot)$ lies outside the uncertainty set, $f_{\text{rel}}^*(\cdot; f_{\text{base}})$ will correspond to the point in $\mathcal{C}(Q_{\mathbf{X}}, \mathcal{H})$ that is closest to $f_{\text{base}}(\cdot)$.

In Sections 4 and 5, we compare the empirical performance of our proposed minimax regret CATE model with the minimax relative-risk CATE model under the standard choice of the zero baseline model. For the construction of the minimax relative-risk CATE estimator, we can similarly use plug-in estimates, as done for the minimax regret estimator (see Section 2.5).

4 Simulation Studies

We conduct simulation studies to evaluate the performance of our proposed minimax regret CATE estimator under various scenarios. To benchmark its performance, we compare it against the pooled CATE estimator, as well as the minimax relative-risk CATE estimator discussed in Section 3. We do not consider the minimax risk estimator given its lack of an identifiable closed-form solution.

4.1 Setup

We generate simulated data from $S = 10$ source sites. For each source site $s \in [S]$, the data generation process is as follows:

$$\begin{aligned} \mathbf{X}_i^{(s)} &\stackrel{\text{i.i.d.}}{\sim} \mathcal{N}(\mathbf{0}, \mathbf{I}_5) \\ A_i^{(s)} &| \mathbf{X}_i^{(s)} \stackrel{\text{i.i.d.}}{\sim} \text{Bernoulli}(0.5) \\ Y_i^{(s)} &= \mu_0^{(s)}(\mathbf{X}_i^{(s)}) + A_i^{(s)} \cdot \tau^{(s)}(\mathbf{X}_i^{(s)}) + \varepsilon_i^{(s)}, \quad \text{where} \quad \varepsilon_i^{(s)} \stackrel{\text{i.i.d.}}{\sim} \mathcal{N}(0, 1). \end{aligned}$$

Here, $\mu_0^{(s)}(\cdot)$ and $\tau^{(s)}(\cdot)$ denote the conditional outcome function under control and the CATE function for site s , respectively. To introduce distributional shifts in treatment effect heterogeneity

across sites, we generate $\mu_0^{(s)}(\cdot)$ and $\tau^{(s)}(\cdot)$ with site-specific parameters. Specifically, we generate the control baseline model as:

$$\mu_0^{(s)}(\mathbf{X}) = \alpha_s X_1 + \sum_{j=2}^5 X_j,$$

where α_s denotes the site-specific parameter to be specified later. For the CATE functions, we consider two distinct settings:

$$\begin{aligned} \text{(A): } \quad & \tau^{(s)}(\mathbf{X}) = \beta_s X_1 \mathbb{1}(X_1 > 0) + 0.2(X_1 X_2 + X_2 X_3), \\ \text{(B): } \quad & \tau^{(s)}(\mathbf{X}) = \begin{cases} \beta_s \cdot 0.6 + \frac{2}{1+\exp(-12(X_1-1/2))} \cdot \frac{2}{1+\exp(-12(X_5-1/2))}, & \text{if } s \in \{1, 2, 3\}, \\ \beta_s \cdot X_1 \mathbb{1}(X_1 > 0) + 0.2(X_1 X_2 + X_2 X_3), & \text{if } s \in \{4, 5, 6\}, \\ \beta_s \cdot 0.5 X_2^2 + 0.3(X_3 + X_4), & \text{if } s \in \{7, 8, 9, 10\}. \end{cases} \end{aligned}$$

In both settings, the coefficient β_s varies across sites to introduce site-specific heterogeneity. Setting A assumes a consistent nonlinear functional form for $\tau^{(s)}$ across all sites, while Setting B considers a more complex scenario with varying functional forms of $\tau^{(s)}$ across sites, creating a more challenging setting, particularly for the pooling approach. This simulation setup is partially adapted from Brantner et al. (2024). The site-specific parameters α_s and β_s are sampled i.i.d from a mixture of normal distributions: $\alpha_s, \beta_s \stackrel{\text{i.i.d.}}{\sim} 0.7 \times \mathcal{N}(0, 0.75^2) + 0.3 \times \mathcal{N}(3, 0.75^2)$.

For a given total sample size n_{total} , each source $s \in [S]$ is allocated a local sample size determined by the sampling weight $q_{\text{mix}} \in \Delta_{S-1}$. Unless stated otherwise, we assume a default sample size of $n_{\text{total}} = 5,000$ and a balanced sample allocation with $q_{\text{mix}} = (\frac{1}{S}, \dots, \frac{1}{S})$. Additionally, we generate target covariate data $\{\mathbf{X}_i^Q\}_{i=1}^{n_Q}$ with a fixed sample size of $n_Q = 10,000$. For simplicity, we assume no covariate shifts between the target and source sites, generating $\mathbf{X}_i^Q \stackrel{\text{i.i.d.}}{\sim} \mathcal{N}(\mathbf{0}, \mathbf{I}_5)$.

For site-specific CATE estimation, we employed multiple methods, including the R-learner and X-learner (Nie and Wager, 2021; Künzel et al., 2019) implemented via the R package `rlearner`, and the causal forest (Wager and Athey, 2018) using the R package `grf`. For the proposed minimax regret and minimax relative-risk estimators, we first computed the aggregation weights by solving the respective QP problems using the R package `CVXR` and then ensembled the source-site CATE estimates to derive the final CATE models. Additionally, we included a pooled CATE estimator, which directly pools all source data together and trains a single CATE model.

To evaluate the robustness of our approach, we will compare the empirical regret of different methods under two settings: (1) the performance on each individual source site distribution, and (2) the *worst-case* regret across all possible target distributions in $\mathcal{C}(Q_{\mathbf{X}})$, which is equivalent to the worst-case regret among the S source sites. According to Equation (6), the empirical regret is measured as the MSE between the estimated CATE model, $\hat{f}(\cdot)$, and a given target CATE, $\tau_Q(\cdot)$, over the target covariate observations: $\frac{1}{n_Q} \sum_{i=1}^{n_Q} (\tau_Q(\mathbf{X}_i^Q) - \hat{f}(\mathbf{X}_i^Q))^2$. For each setup, we conduct 1,000 Monte Carlo simulations.

4.2 Results

Before presenting the main results, we note that in the current settings, all base single-site CATE estimation methods (R-learner, X-learner, and causal forest) perform reasonably well and yield similar final multisite CATE estimates. Therefore, we report the results based on the R-learner in the main text, with additional results for the X-learner and causal forest provided in Appendix D.1.

We first examine the performance of different CATE estimators on each individual source site. Figure 1 presents the regret averaged across simulations for each method under both Set-

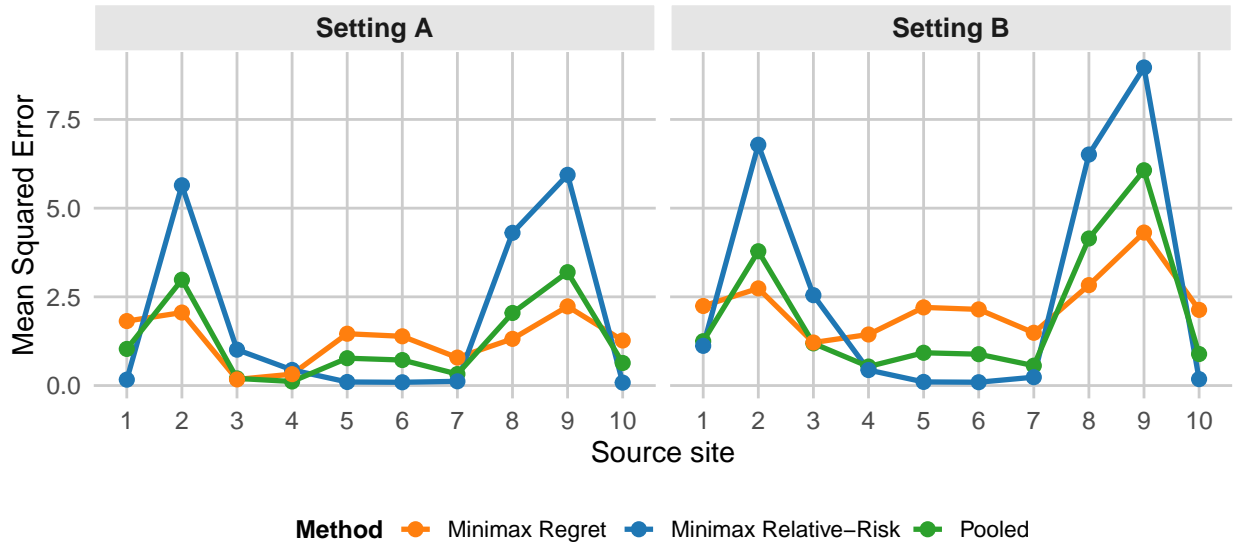


Figure 1: Average MSE of multisite CATE estimates from three methods across 1,000 simulations, evaluated over different source sites, using R-learner as the site-specific CATE estimation method.

tings A and B. Our proposed minimax regret estimator (orange) demonstrates robust performance across diverse source sites, when compared to the minimax relative-risk (blue) and pooled (green) estimators. Specifically, it achieves lower prediction error on key “boundary” sites (e.g., sites 2, 8, and 9) and attains the overall lowest worst-case error across all sites. This aligns with its design to handle worst-case scenarios effectively. In contrast, the minimax relative-risk estimator, while optimized for robustness against a zero-constant baseline model, tends to be overly conservative, resulting in significantly poor performance on certain sites. Similarly, the pooled method lacks worst-case robustness guarantees, as it fails to account for target distributions that deviate from the pooled source distribution.

Setting B introduces greater heterogeneity across sites by allowing varying functional forms for the CATE, in contrast to the consistent functional forms in Setting A. This increased heterogeneity amplifies the difficulty of learning a generalizable CATE model across diverse target distributions, resulting in higher worst-case regret for all methods. While the relative performance ranking remains the same as before, the pooled and relative-risk estimators show greater vulnerability to this functional heterogeneity. The performance of the pooled estimator, in particular, becomes worse as the single pooled model struggles to perform well when functional forms differ significantly across sites.

In comparison, the minimax regret approach maintains robust performance, with smaller variation and better error control across sites than the other methods. These findings emphasize the adaptability of the proposed estimator to complex cross-site heterogeneity while providing strong worst-case guarantees. As a result, the minimax regret approach offers a consistent advantage in addressing the challenges posed by heterogeneous settings.

We also evaluate the impact of imbalanced sample sizes of source sites on the performance of each method. We simulate three scenarios with a total sample size of $n_{\text{total}} = 5000$: (1) “Balanced”: all sites have an equal sample size, (2) “Half-and-half”: half of the sites have three times the sample size of the others, with larger samples either in the first or the second half, and (3) “One Large”: one site has a sample size 10 times larger than the others, with the largest site being either the 1st

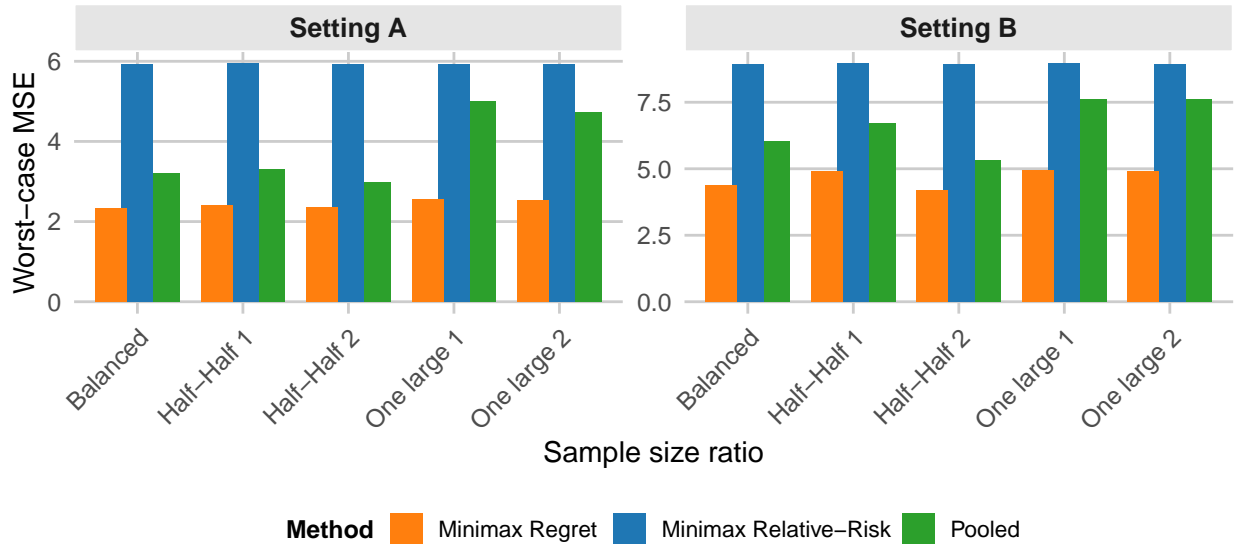


Figure 2: Worst-case MSE averaged across 1,000 iterations under varying sample size ratios: (1) **Balanced**: all sites have equal sample sizes, (2) **Half-and-Half**: half of the sites have three times the sample size of the others, and (3) **One Large**: one site has a sample size 10 times larger than the others. For scenarios (2) and (3), we evaluate two configurations, each with a different subset of large sites. We use R-learner for site-specific CATE estimation.

or the 5th site.

As shown in Figure 2, the pooled estimator is highly sensitive to the imbalances of site sample sizes, with its performance heavily influenced by the large sites. This sensitivity arises because the pooled method weights sites proportionally to their sample sizes. When site sample sizes vary significantly, the pooled estimator becomes dominated by the larger sites, leading to biased estimates and poor generalization to smaller sites or target distributions.

By contrast, the minimax regret and minimax relative-risk estimators demonstrate robust performance across all configurations. These methods remain stable even in the presence of substantial sample size imbalances, though the minimax relative-risk estimator is too conservative and performs worst in terms of MSE. This robustness comes from the ability to balance contributions from all source sites, mitigating the disproportionate influence of large sites. Each site contributes appropriately to the final CATE estimate based on how much its CATE differs from others, as reflected in the robust optimization objective, as long as the site has enough samples to reliably estimate its local CATE. The results highlight the advantage of the minimax regret estimator in scenarios with heterogeneous sample sizes, as it avoids the pitfalls of oversampling bias inherent in the pooled approach.

5 Empirical Application: Microcredit Experiments

5.1 Background and Setup

To illustrate our proposed method, we turn to a set of microcredit experiments. These experiments were carried out in different geographic regions around the world – Morocco, Bosnia and Herzegovina, Mexico, and Mongolia – with the aim of evaluating whether microcredit fosters entrepreneur-

ship among poor households (e.g., [Roodman, 2012](#)). Within each experiment, participants were randomly provided with increased access to credit from a Microfinance Institution (MFI). However, because the geographic regions in which these experiments took place were so different and because the specifics of each experimental design varied, there is a great degree of heterogeneity across the different experiments ([Meager, 2019](#)).

For example, the experiment in Bosnia ([Augsburg et al., 2015](#)) randomized whether individuals who would otherwise be marginally rejected were provided loans. In contrast, other studies chose random communities to open a branch of an MFI for easier access. This implies that in addition to the differences between sites in the assigned treatment, the contexts vary considerably between the different experiments. The studies also vary in terms of the MFI’s relationship with the local community. For example, in the study conducted by [Augsburg et al. \(2015\)](#), the MFI was already operating locally, before the experiment. In contrast, the experiments conducted in [Angelucci et al. \(2015\)](#); [Attanasio et al. \(2015\)](#); [Crépon et al. \(2015\)](#) considered MFI’s that were not previously operating locally. We summarize the details of each experimental site in Appendix Table [D.1](#).

We consider four scenarios that synthetically generate target populations to mimic the types of distributional shifts researchers may encounter in practice. Specifically, empirical target distributions are constructed by resampling from the original source site data, with the total number of target observations held constant across all scenarios.

1. *Pooled source distribution.* The target distribution is identical to the pooled source distribution, with mixture weights proportional to the sample sizes of the original source sites.
2. *Equally weighted distribution.* The target distribution is a mixture of all source distributions with equal weights.
3. *Single site dominated distribution.* The target distribution is primarily dominated by a single source site, mimicking a scenario in which the target population closely resembles subsets of the source sites. The sampling weights are set as $(\frac{5}{8}, \frac{1}{8}, \frac{1}{8}, \frac{1}{8})$, with one site contributing $\frac{5}{8}$ of the target population and the remaining three sites contributing $\frac{1}{8}$ each.
4. *Two sites dominated distribution.* The target distribution is dominated by two source sites, each contributing 40% of the weight, while the remaining two sites contribute 10% each.

Within each source site, we fit a CATE model using Causal Forest ([Wager and Athey, 2018](#)). To evaluate the robustness of our minimax regret approach, we compare its performance against benchmark methods, including the minimax relative-risk and pooled approaches, across the different target distributions. We treat the oracle CATE as the weighted average of source-site CATEs.

5.2 Results

Overall, the minimax regret approach ensures the best worst-case performance across the various scenarios. Additionally, even when evaluating individual scenarios separately, the minimax regret approach generally outperforms both the pooling and minimax relative-risk methods.

Table [1](#) presents the results in terms of MSE. In Scenario 1 (Pooled source distribution), as expected, the pooled approach achieves the lowest MSE by perfectly aligning with the target distribution. In Scenario 2 (Equally weighted distribution), however, due to the imbalance in the original source sample sizes, the pooled approach performs worse than the minimax regret method. The minimax relative-risk approach performs poorly in both scenarios because its solution aims to minimize the distance to the conservative baseline model, causing it to overweight the CATE model to the most extreme source distribution.

| | Pooled | Regret | Relative-risk |
|-----------------------------------|---------------|---------------|----------------|
| Scenario 1: | | | |
| Equivalent to Source Distribution | 161.95 | 370.31 | 4487.17 |
| Scenario 2: | | | |
| Equal Weight | 228.27 | 28.30 | 1893.92 |
| Scenario 3: | | | |
| Mexico | 503.19 | 205.60 | 1150.71 |
| Mongolia | 963.35 | 563.68 | 463.06 |
| Bosnia | 165.08 | 69.09 | 2575.35 |
| Morocco | 215.86 | 479.48 | 4878.23 |
| Scenario 4: | | | |
| Mexico & Mongolia | 844.07 | 461.41 | 603.72 |
| Mexico & Bosnia | 282.82 | 70.00 | 1775.48 |
| Mexico & Morocco | 112.19 | 44.70 | 2691.45 |
| Mongolia & Bosnia | 471.47 | 156.40 | 1210.93 |
| Mongolia & Morocco | 168.86 | 4.62 | 2041.46 |
| Bosnia & Morocco | 125.95 | 276.24 | 4082.04 |

Table 1: The results in terms of MSE for each method. Bolded entries indicate the best-performing method with the lowest error within each scenario (i.e., minimum value for each row), while red entries highlight the worst-case error for each method across *all* scenarios (i.e., maximum value for each column).

In Scenario 3 (Single site dominated distribution) across most settings, the pooled approach performs poorly because its implicit weighting reflects the observed sample, which does not align well with the target distribution. The only exception is the case where Morocco dominates the target distribution. This is because Morocco has the largest sample size in the source data, making this specific setting closer to the complete pooling distribution.

In general, the minimax regret approach also outperforms the relative-risk approach in most cases. The exception occurs in the setting where the target distribution is dominated by Mongolia, the most extreme source distribution with a CATE closest to zero baseline. In this case, the minimax relative-risk approach performs better, as its conservativeness ensures good performance in this extreme setting. We observe a similar pattern in Scenario 4, in which the target distribution is dominated by two of the sites.

Additionally, we evaluate how well the estimated models adapt to the different target population distributions. Specifically, we compare the aggregation weights in the final minimax CATE model estimated by each method across the different scenarios. For comparison, we report the weights for the pooled approach as the original source sample size ratios, which remain fixed regardless of the target distribution. Although both the minimax relative-risk and minimax regret approaches theoretically produce aggregation weights that depend on the target covariate distribution, empirically, the weights do not vary significantly across different target scenarios. Specifically, the estimated weights for the minimax relative-risk approach are consistently dominated by a single site (Mongolia), whereas the minimax regret approach assigns non-zero weights across two different source distributions (Mongolia and Morocco). See Appendix Figure D.5 for visualization of the weights.

In summary, our proposed minimax regret approach demonstrates both robustness and adaptability in real-world multisite settings. It guarantees robust performance across a broad range of target distributions, outperforming the naive pooled method, especially in scenarios with significant heterogeneity across sites, while being less conservative than the minimax relative-risk approach, which is heavily influenced by the pre-specified baseline.

6 Concluding Remarks

In this paper, we develop a minimax regret framework to learn a generalizable CATE model across heterogeneous multisite data. We formulate the problem as a minimax counterfactual prediction task and leverage the regret criterion under the assumption that an unknown target CATE model can be modeled as a convex mixture of source site CATE models. We demonstrate that the proposed minimax regret CATE model is robust to unknown distributional shifts in treatment effect and provides performance guarantees across a wide range of target populations. We further show that the robust CATE model admits an interpretable closed-form solution. This approach is computationally efficient, enables the use of flexible off-the-shelf CATE estimation methods to obtain site-specific estimates, and avoids sharing individual-level data across sites when computing the robust CATE model.

There are several future directions to build on the proposed framework. This work focuses on the continuous outcome setting, using squared error loss in the regret criterion. An interesting extension would be to apply the framework to classification settings, where the outcome variable is categorical. Although the minimax regret framework for robust CATE estimation could still be applicable, the closed-form solution derived in this paper may not generalize, requiring the development of new techniques to solve the optimization problem.

Furthermore, our approach implicitly assumes that all sites share the same set of covariates for the estimation of CATE. In practice, however, the measurement of the same constructs can differ across sites while some sites may completely lack key covariates, creating challenges such as discordant measurements or systematic missing data (Brantner et al., 2023). Addressing these issues is an important direction to further enhance the robustness and generalizability of CATE estimation across multiple sites. Another interesting avenue for future research is to consider how to use multiple source sites to help mitigate potential concerns about overlap violations between the sources and the target population.

References

- Agarwal, A. and T. Zhang (2022). Minimax regret optimization for robust machine learning under distribution shift. In *Conference on Learning Theory*, pp. 2704–2729. PMLR.
- Angelucci, M., D. Karlan, and J. Zinman (2015). Microcredit impacts: Evidence from a randomized microcredit program placement experiment by compartamos banco. *American Economic Journal: Applied Economics* 7(1), 151–182.
- Attanasio, O., B. Augsburg, R. De Haas, E. Fitzsimons, and H. Harmgart (2015). The impacts of microfinance: Evidence from joint-liability lending in mongolia. *American Economic Journal: Applied Economics* 7(1), 90–122.
- Augsburg, B., R. De Haas, H. Harmgart, and C. Meghir (2015). The impacts of microcredit: Evidence from bosnia and herzegovina. *American Economic Journal: Applied Economics* 7(1), 183–203.
- Awasthi, P., N. Haghtalab, and E. Zhao (2023). Open problem: The sample complexity of multi-distribution learning for vc classes. In *The Thirty Sixth Annual Conference on Learning Theory*, pp. 5943–5949. PMLR.
- Bareinboim, E. and J. Pearl (2016). Causal inference and the data-fusion problem. *Proceedings of the National Academy of Sciences* 113(27), 7345–7352.
- Ben-Michael, E., D. J. Greiner, K. Imai, and Z. Jiang (2021). Safe policy learning through extrapolation: Application to pre-trial risk assessment. *arXiv preprint arXiv:2109.11679*.
- Ben-Tal, A., D. Den Hertog, A. De Waegenare, B. Melenberg, and G. Rennen (2013). Robust solutions of optimization problems affected by uncertain probabilities. *Management Science* 59(2), 341–357.
- Brantner, C. L., T.-H. Chang, T. Q. Nguyen, H. Hong, L. Di Stefano, and E. A. Stuart (2023). Methods for integrating trials and non-experimental data to examine treatment effect heterogeneity. *Statistical science: a review journal of the Institute of Mathematical Statistics* 38(4), 640.
- Brantner, C. L., T. Q. Nguyen, T. Tang, C. Zhao, H. Hong, and E. A. Stuart (2024). Comparison of methods that combine multiple randomized trials to estimate heterogeneous treatment effects. *Statistics in Medicine*.
- Burke, D. L., J. Ensor, and R. D. Riley (2017). Meta-analysis using individual participant data: one-stage and two-stage approaches, and why they may differ. *Statistics in medicine* 36(5), 855–875.
- Carranza, A. G. and S. Athey (2024). Robust offline policy learning with observational data from multiple sources. *arXiv preprint arXiv:2410.08537*.
- Cheng, D. and T. Cai (2021). Adaptive combination of randomized and observational data. *arXiv preprint arXiv:2111.15012*.
- Crépon, B., F. Devoto, E. Duflo, and W. Parienté (2015). Estimating the impact of microcredit on those who take it up: Evidence from a randomized experiment in morocco. *American Economic Journal: Applied Economics* 7(1), 123–150.

- Curth, A., D. Svensson, J. Weatherall, and M. van der Schaar (2021). Really doing great at estimating cate? a critical look at ml benchmarking practices in treatment effect estimation. In *Thirty-fifth conference on neural information processing systems datasets and benchmarks track (round 2)*.
- Curth, A. and M. Van der Schaar (2021). Nonparametric estimation of heterogeneous treatment effects: From theory to learning algorithms. In *International Conference on Artificial Intelligence and Statistics*, pp. 1810–1818. PMLR.
- Dahabreh, I. J. and M. A. Hernán (2019). Extending inferences from a randomized trial to a target population. *European journal of epidemiology* 34, 719–722.
- Dahabreh, I. J., S. E. Robertson, L. C. Petito, M. A. Hernán, and J. A. Steingrimsson (2023). Efficient and robust methods for causally interpretable meta-analysis: Transporting inferences from multiple randomized trials to a target population. *Biometrics* 79(2), 1057–1072.
- Debray, T. P., K. G. Moons, G. van Valkenhoef, O. Efthimiou, N. Hummel, R. H. Groenwold, J. B. Reitsma, and G. M. R. Group (2015). Get real in individual participant data (ipd) meta-analysis: a review of the methodology. *Research synthesis methods* 6(4), 293–309.
- Deng, Y., M. M. Kamani, and M. Mahdavi (2020). Distributionally robust federated averaging. *Advances in neural information processing systems* 33, 15111–15122.
- Dorn, J., K. Guo, and N. Kallus (2024). Doubly-valid/doubly-sharp sensitivity analysis for causal inference with unmeasured confounding. *Journal of the American Statistical Association*, 1–12.
- Duchi, J. C., P. W. Glynn, and H. Namkoong (2021). Statistics of robust optimization: A generalized empirical likelihood approach. *Mathematics of Operations Research* 46(3), 946–969.
- Duchi, J. C. and H. Namkoong (2021). Learning models with uniform performance via distributionally robust optimization. *The Annals of Statistics* 49(3), 1378–1406.
- Egami, N. and E. Hartman (2023). Elements of external validity: Framework, design, and analysis. *American Political Science Review* 117(3), 1070–1088.
- Egami, N. and D. D. I. Lee (2024). Designing multi-site studies for external validity: Site selection via synthetic purposive sampling. *Available at SSRN 4717330*.
- Elzinga, D. J. and D. W. Hearn (1972). The minimum covering sphere problem. *Management science* 19(1), 96–104.
- Guo, Z. (2023). Statistical inference for maximin effects: Identifying stable associations across multiple studies. *Journal of the American Statistical Association*, 1–17.
- Hahn, P. R., J. S. Murray, and C. M. Carvalho (2020). Bayesian regression tree models for causal inference: Regularization, confounding, and heterogeneous effects (with discussion). *Bayesian Analysis* 15(3), 965–1056.
- Hastings, J., C. Jung, C. Peale, and V. Syrgkanis (2024). Taking a moment for distributional robustness. *arXiv preprint arXiv:2405.05461*.
- Hatt, T., J. Berrevoets, A. Curth, S. Feuerriegel, and M. van der Schaar (2022). Combining observational and randomized data for estimating heterogeneous treatment effects. *arXiv preprint arXiv:2202.12891*.

- Hu, W., G. Niu, I. Sato, and M. Sugiyama (2018). Does distributionally robust supervised learning give robust classifiers? In *International Conference on Machine Learning*, pp. 2029–2037. PMLR.
- Huang, M. (2024+a). Overlap violations in external validity. *Annals of Applied Statistics (Forthcoming)*.
- Huang, M., N. Egami, E. Hartman, and L. Miratrix (2023). Leveraging population outcomes to improve the generalization of experimental results: Application to the jtpa study. *The Annals of Applied Statistics* 17(3), 2139–2164.
- Huang, M. Y. (2024b). Sensitivity analysis for the generalization of experimental results. *Journal of the Royal Statistical Society Series A: Statistics in Society*, qnae012.
- Imai, K. and M. Ratkovic (2013). Estimating treatment effect heterogeneity in randomized program evaluation.
- Ishihara, T. and T. Kitagawa (2021). Evidence aggregation for treatment choice. *arXiv preprint arXiv:2108.06473*.
- Jin, Y., Z. Ren, and Z. Zhou (2022). Sensitivity analysis under the f -sensitivity models: a distributional robustness perspective. *arXiv preprint arXiv:2203.04373*.
- Kallus, N. and A. Zhou (2018). Confounding-robust policy improvement. *Advances in neural information processing systems* 31.
- Kallus, N. and A. Zhou (2021). Minimax-optimal policy learning under unobserved confounding. *Management Science* 67(5), 2870–2890.
- Kennedy, E. H. (2023). Towards optimal doubly robust estimation of heterogeneous causal effects. *Electronic Journal of Statistics* 17(2), 3008–3049.
- Kern, C., M. Kim, and A. Zhou (2024). Multi-cate: Multi-accurate conditional average treatment effect estimation robust to unknown covariate shifts. *arXiv preprint arXiv:2405.18206*.
- Kido, D. (2022). Distributionally robust policy learning with wasserstein distance. *arXiv preprint arXiv:2205.04637*.
- Künzel, S. R., J. S. Sekhon, P. J. Bickel, and B. Yu (2019). Metalearners for estimating heterogeneous treatment effects using machine learning. *Proceedings of the national academy of sciences* 116(10), 4156–4165.
- Lei, L., R. Sahoo, and S. Wager (2023). Policy learning under biased sample selection. *arXiv preprint arXiv:2304.11735*.
- Manski, C. F. (2004). Statistical treatment rules for heterogeneous populations. *Econometrica* 72(4), 1221–1246.
- Manski, C. F. (2011). Choosing treatment policies under ambiguity. *Annu. Rev. Econ.* 3(1), 25–49.
- Meager, R. (2019). Understanding the average impact of microcredit expansions: A bayesian hierarchical analysis of seven randomized experiments. *American Economic Journal: Applied Economics* 11(1), 57–91.
- Meinshausen, N. and P. Bühlmann (2015). Maximin effects in inhomogeneous large-scale data.

- Miratrix, L. W., M. J. Weiss, and B. Henderson (2021). An applied researcher’s guide to estimating effects from multisite individually randomized trials: Estimands, estimators, and estimates. *Journal of Research on Educational Effectiveness* 14(1), 270–308.
- Mo, W., Z. Qi, and Y. Liu (2021). Learning optimal distributionally robust individualized treatment rules. *Journal of the American Statistical Association* 116(534), 659–674.
- Mo, W., W. Tang, S. Xue, Y. Liu, and J. Zhu (2024). Minimax regret learning for data with heterogeneous subgroups. *arXiv preprint arXiv:2405.01709*.
- Nguyen, T. Q., C. Ebnesaajjad, S. R. Cole, and E. A. Stuart (2017). Sensitivity analysis for an unobserved moderator in rct-to-target-population generalization of treatment effects. *The Annals of Applied Statistics*, 225–247.
- Nie, X., G. Imbens, and S. Wager (2021). Covariate balancing sensitivity analysis for extrapolating randomized trials across locations. *arXiv preprint arXiv:2112.04723*.
- Nie, X. and S. Wager (2021). Quasi-oracle estimation of heterogeneous treatment effects. *Biometrika* 108(2), 299–319.
- Roodman, D. (2012). *Due diligence: An impertinent inquiry into microfinance*. CGD Books.
- Rubin, D. B. (1990). Comment: Neyman (1923) and causal inference in experiments and observational studies. *Statistical Science* 5(4), 472–480.
- Sagawa, S., P. W. Koh, T. B. Hashimoto, and P. Liang (2019). Distributionally robust neural networks for group shifts: On the importance of regularization for worst-case generalization. *arXiv preprint arXiv:1911.08731*.
- Savage, L. J. (1951). The theory of statistical decision. *Journal of the American Statistical Association* 46(253), 55–67.
- Seo, M., I. R. White, T. A. Furukawa, H. Imai, M. Valgimigli, M. Egger, M. Zwahlen, and O. Efthimiou (2021). Comparing methods for estimating patient-specific treatment effects in individual patient data meta-analysis. *Statistics in medicine* 40(6), 1553–1573.
- Shalit, U., F. D. Johansson, and D. Sontag (2017). Estimating individual treatment effect: generalization bounds and algorithms. In *International conference on machine learning*, pp. 3076–3085. PMLR.
- Shyr, C., B. Ren, P. Patil, and G. Parmigiani (2023). Multi-study r-learner for estimating heterogeneous treatment effects across studies using statistical machine learning. *arXiv e-prints*, arXiv–2306.
- Stoye, J. (2012). Minimax regret treatment choice with covariates or with limited validity of experiments. *Journal of Econometrics* 166(1), 138–156.
- Stuart, E. A., C. P. Bradshaw, and P. J. Leaf (2015). Assessing the generalizability of randomized trial results to target populations. *Prevention Science* 16, 475–485.
- Tan, X., C.-C. H. Chang, L. Zhou, and L. Tang (2022). A tree-based model averaging approach for personalized treatment effect estimation from heterogeneous data sources. In *International Conference on Machine Learning*, pp. 21013–21036. PMLR.

- Tipton, E. and M. Mamakos (2023). Designing randomized experiments to predict unit-specific treatment effects. *arXiv preprint arXiv:2310.18500*.
- Wager, S. and S. Athey (2018). Estimation and inference of heterogeneous treatment effects using random forests. *Journal of the American Statistical Association* 113(523), 1228–1242.
- Wang, Z., P. Bühlmann, and Z. Guo (2023). Distributionally robust machine learning with multi-source data. *arXiv preprint arXiv:2309.02211*.
- Wolfe, P. (1961). A duality theorem for non-linear programming. *Quarterly of applied mathematics* 19(3), 239–244.
- Yadlowsky, S., H. Namkoong, S. Basu, J. Duchi, and L. Tian (2018). Bounds on the conditional and average treatment effect with unobserved confounding factors. *arXiv preprint arXiv:1808.09521*.
- Yang, S., C. Gao, D. Zeng, and X. Wang (2023). Elastic integrative analysis of randomised trial and real-world data for treatment heterogeneity estimation. *Journal of the Royal Statistical Society Series B: Statistical Methodology* 85(3), 575–596.
- Zhang, Z., W. Zhan, Y. Chen, S. S. Du, and J. D. Lee (2023). Optimal multi-distribution learning. *arXiv preprint arXiv:2312.05134*.

Supplementary Appendix

A Closed-Form Minimax Squared-error CATE Estimator

We derive a closed-form solution for the minimax estimator based on the squared-error objective, under the special case where $S = 2$ and an additional assumption on the target distribution. Specifically, we restrict the target distribution Q to the following uncertainty set:

$$\tilde{\mathcal{C}}(Q_{\mathbf{X}}) := \left\{ Q = (Q_{\mathbf{X}}, Q_{(Y(1), Y(0))|\mathbf{X}}) \mid Q_{Y(1)-Y(0)|\mathbf{X}} = \sum_{s=1}^S q_s \cdot P_{Y(1)-Y(0)|\mathbf{X}}^{(s)} \quad \text{with } \mathbf{q} \in \Delta_{S-1} \right\}. \quad (\text{A.1})$$

Notably, this restricted uncertainty set $\tilde{\mathcal{C}}(Q_{\mathbf{X}})$ is a subset of the uncertainty set $\mathcal{C}(Q_{\mathbf{X}})$ considered in the main text. It further constrains the entire target conditional treatment effect distribution $Q_{Y(1)-Y(0)|\mathbf{X}}$ to be a convex combination of the source site distributions $\left\{ P_{Y(1)-Y(0)|\mathbf{X}}^{(s)} \right\}_{s=1}^S$.

Now, we derive a closed-form solution for f_{risk}^* in Equation (13) when optimizing over the restricted uncertainty set $\tilde{\mathcal{C}}(Q_{\mathbf{X}})$.

Proposition A.1. Suppose $S = 2$. Define $\varepsilon_i^{(s)} := Y_i^{(s)}(1) - Y_i^{(s)}(0) - \tau^{(s)}(\mathbf{X}_i^{(s)})$ for $s = 1, 2$. Assume $\tau^{(1)} \neq \tau^{(2)}$, $\mathbb{E}_{P^{(1)}} \left[\left(\varepsilon_i^{(1)} \right)^2 \mid \mathbf{X}_i^{(1)} \right] = \sigma_1^2$ and $\mathbb{E}_{P^{(2)}} \left[\left(\varepsilon_i^{(2)} \right)^2 \mid \mathbf{X}_i^{(2)} \right] = \sigma_2^2$, and $\varepsilon_i^{(s)}$ being independent of $\mathbf{X}_i^{(s)}$ for $s \in [S]$. Then, f_{risk}^* in Equation (13), optimized over $\tilde{\mathcal{C}}(Q_{\mathbf{X}})$, can be written as:

$$f_{\text{risk}}^* = q_1^* \tau^{(1)} + (1 - q_1^*) \tau^{(2)} \quad \text{with} \quad q_1^* = 0 \vee \left(\frac{1}{2} + \frac{\sigma_1^2 - \sigma_2^2}{2 \|\tau^{(1)} - \tau^{(2)}\|_{Q_{\mathbf{X},2}}^2} \right) \wedge 1,$$

where $\|\cdot\|_{Q_{\mathbf{X},2}}$ is defined as the L_2 -norm measured over the target covariate distribution $Q_{\mathbf{X}}$.

The proof is omitted because the result follows from Proposition 2 of Wang et al. (2023) by applying their standard statistical learning framework to the current causal context. Proposition A.1 implies that f_{risk}^* can be expressed in closed form as a convex combination of the site-specific CATEs, $\tau^{(1)}$ and $\tau^{(2)}$. The estimator, however, is less robust than our proposed minimax regret estimator f_{regret}^* . Specifically, when noise levels are homogeneous between the two sites, i.e., $\sigma_1^2 = \sigma_2^2$, f_{risk}^* is the equal average of $\tau^{(1)}$ and $\tau^{(2)}$, which equals f_{regret}^* . In contrast, in the case of heterogeneous noise levels, f_{risk}^* becomes sensitive to the noisier site. For example, when one site has a significantly higher level of noise than the other, i.e., $\sigma_1^2 \gg \sigma_2^2$, f_{risk}^* is dominated by $\tau^{(1)}$. This result aligns with the intuition based on Equation (14), where f_{risk}^* primarily optimizes prediction performance for the site with higher noise.

B Convergence Rates for CATE Estimators

We characterize δ_n for specific examples of CATE estimators. For clarity, we omit the superscript site indicator s in the following examples and let n denote the generic sample size of a given site. Define a function as p -smooth if it has p continuous and bounded derivatives. Assume the following

smoothness conditions for each function:

$$\begin{aligned}\mu_a(\mathbf{x}) &:= \mathbb{E}[Y(a) \mid \mathbf{X} = \mathbf{x}] \text{ is } p_{\mu_a}\text{-smooth,} \\ \pi(\mathbf{x}) &:= \mathbb{P}(A = 1 \mid \mathbf{X} = \mathbf{x}) \text{ is } p_{\pi}\text{-smooth,} \\ \tau(\mathbf{x}) &:= \mu_1(\mathbf{x}) - \mu_0(\mathbf{x}) \text{ is } p_{\tau}\text{-smooth.}\end{aligned}$$

Assume further that each of these functions is estimable at a minimax rate of $n^{\frac{-p_i}{2p_i+d}}$, where p_i corresponds to the smoothness level of the respective function, and d is the dimension of covariates. Table B.1 gives the error bound of some commonly used meta-learners.

| Estimator | δ_n rate |
|--|--|
| T-learner (Künzel et al., 2019) | $O\left(n^{\frac{-p_{\mu_0}}{2p_{\mu_0}+d}} + n^{\frac{-p_{\mu_1}}{2p_{\mu_1}+d}}\right)$ |
| X-learner (Künzel et al., 2019) | $O\left(n^{\frac{-p_{\tau}}{2p_{\tau}+d}} + n^{\frac{-p_{\mu_0}}{2p_{\mu_0}+d}} + n^{\frac{-p_{\mu_1}}{2p_{\mu_1}+d}}\right)$ |
| DR-learner (Kennedy, 2023) | $O\left(n^{\frac{-p_{\tau}}{2p_{\tau}+d}} + n^{-\left(\min_a \frac{p_{\mu_a}}{2p_{\mu_a}+d} + \frac{p_{\pi}}{2p_{\pi}+d}\right)}\right)$ |

Table B.1: Examples of δ_n for Different CATE Estimators. Note: If $\min_a \frac{p_{\mu_a}}{2p_{\mu_a}+d} + \frac{p_{\pi}}{2p_{\pi}+d} > \frac{p_{\tau}}{2p_{\tau}+d}$, the DR-learner achieves the oracle rate $n^{\frac{-p_{\tau}}{2p_{\tau}+d}}$.

C Proofs

Additional Notation. The ℓ_q norm of a p -dimensional vector v is defined as $\|v\|_q = \left(\sum_{l=1}^p |v_l|^q\right)^{\frac{1}{q}}$ for $q \geq 0$ and $\|v\|_{\infty} = \max_{1 \leq l \leq p} |v_l|$. For a matrix A , we use $\lambda_j(A)$, $\|A\|_F$, $\|A\|_2$ and $\|A\|_{\infty}$ to denote its j -th largest singular value, Frobenius norm, spectral norm, and element-wise maximum norm, respectively.

C.1 Proof of Proposition 1

The proof of Equation (8) is included in Appendix C.2 as an intermediate result for proving Theorem 1. Here, we prove Equation (7).

Proof. By definition of minimax optimization, Equation (6) is equivalent to

$$\begin{aligned}(f_{\text{regret}}^*, R^*) &:= \arg \min_{f \in \mathcal{F}, R \in \mathbb{R}} R \\ &\text{subject to } \mathbb{E}_{Q_{\mathbf{X}}}[(f(\mathbf{X}) - \tau_Q(\mathbf{X}))^2] \leq R \quad \text{for all } Q \in \mathcal{C}(Q_{\mathbf{X}}).\end{aligned}\tag{C.1}$$

Since each target CATE can be expressed as a weighted average of site-specific CATEs, we only need to show that for any given R and f ,

$$\begin{aligned}&\left\{ \mathbb{E}_{Q_{\mathbf{X}}} \left[\left(f(\mathbf{X}) - \sum_{s=1}^S q_s \cdot \tau^{(s)}(\mathbf{X}) \right)^2 \right] \leq R, \quad \mathbf{q} \in \Delta_{S-1} \right\} \\ &= \left\{ \mathbb{E}_{Q_{\mathbf{X}}} [(f(\mathbf{X}) - \tau^{(s)}(\mathbf{X}))^2] \leq R, \quad s \in [S] \right\}.\end{aligned}$$

It then suffices to show that, for any $\mathbf{q} \in \Delta_{S-1}$, the following holds:

$$\mathbb{E}_{Q_{\mathbf{X}}} \left[\left(f(\mathbf{X}) - \sum_{s=1}^S q_s \cdot \tau^{(s)}(\mathbf{X}) \right)^2 \right] \leq \max_{s \in [S]} \mathbb{E}_{Q_{\mathbf{X}}} [(f(\mathbf{X}) - \tau^{(s)}(\mathbf{X}))^2].$$

We can show this as follows:

$$\begin{aligned} \mathbb{E}_{Q_{\mathbf{X}}} \left[\left(f(\mathbf{X}) - \sum_{s=1}^S q_s \cdot \tau^{(s)}(\mathbf{X}) \right)^2 \right] &= \mathbb{E}_{Q_{\mathbf{X}}} \left[f^2(\mathbf{X}) - 2f(\mathbf{X}) \sum_{s=1}^S q_s \cdot \tau^{(s)}(\mathbf{X}) \right] + \mathbb{E}_{Q_{\mathbf{X}}} \left[\left(\sum_{s=1}^S q_s \cdot \tau^{(s)}(\mathbf{X}) \right)^2 \right] \\ &\leq \mathbb{E}_{Q_{\mathbf{X}}} \left[f^2(\mathbf{X}) - 2f(\mathbf{X}) \sum_{s=1}^S q_s \cdot \tau^{(s)}(\mathbf{X}) \right] + \mathbb{E}_{Q_{\mathbf{X}}} \left[\sum_{s=1}^S q_s \cdot \left(\tau^{(s)}(\mathbf{X}) \right)^2 \right] \\ &= \sum_{s=1}^S q_s \cdot \mathbb{E}_{Q_{\mathbf{X}}} [(f(\mathbf{X}) - \tau^{(s)}(\mathbf{X}))^2] \\ &\leq \max_{s \in [S]} \mathbb{E}_{Q_{\mathbf{X}}} [(f(\mathbf{X}) - \tau^{(s)}(\mathbf{X}))^2], \end{aligned}$$

where the inequality in the second line is due to $\mathbf{q} \in \Delta_{S-1}$ and the Cauchy-Schwarz inequality, which ensures that $\left(\sum_{s=1}^S q_s \cdot \tau^{(s)}(\mathbf{X}) \right)^2 \leq \left(\sum_{s=1}^S q_s \right) \left(\sum_{s=1}^S q_s \cdot \left(\tau^{(s)}(\mathbf{X}) \right)^2 \right)$ holds pointwise for every value of \mathbf{X} . Thus, we have shown that Equation (C.1) is equivalent to Equation (7). \square

C.2 Proof of Theorem 1

Since the model class \mathcal{F} contains the true CATE models $\tau_Q(\cdot)$ for all $Q \in \mathcal{C}(Q_{\mathbf{X}})$, as noted at the beginning of Section 2.3, the original minimax regret optimization problem in Equation (5) can be equivalently reformulated as the minimax MSE optimization problem in Equation (6). Therefore, by the first part of Proposition 1, we can focus on solving the optimization problem given in Equation (7), which we refer to as the primal problem.

To complete the proof, we leverage the results from Elzinga and Hearn (1972), which provide a closed-form solution for the special case where \mathcal{F} is a linear model class. We extend their proof by using functional analysis so that we can accommodate a more general model class \mathcal{F} within the $L_2(Q_{\mathbf{X}})$ Hilbert space.

Proof. We begin by noting that Equation (7) is a convex optimization problem. To see this clearly, we consider $\lambda \in [0, 1]$ and any $f_1, f_2 \in \mathcal{F}$. We can verify that $\mathbb{E}_{Q_{\mathbf{X}}} [(\lambda f_1(\mathbf{X}) + (1 - \lambda)f_2(\mathbf{X}) - \tau^{(s)}(\mathbf{X}))^2] \leq \lambda \mathbb{E}_{Q_{\mathbf{X}}} [(f_1(\mathbf{X}) - \tau^{(s)}(\mathbf{X}))^2] + (1 - \lambda) \mathbb{E}_{Q_{\mathbf{X}}} [(f_2(\mathbf{X}) - \tau^{(s)}(\mathbf{X}))^2]$ for all $s \in [S]$. Moreover, the Slater constraint qualification is clearly satisfied since there exist feasible $f_0 \in \mathcal{F}$ and $R_0 \in \mathbb{R}$ that strictly satisfy the inequality constraint.

Therefore, the Karush-Kuhn-Tucker conditions give a satisfying characterization of both necessary and sufficient optimality conditions for Equation (7). Specifically, there exist multipliers

q_1^*, \dots, q_S^* such that

$$\sum_{s=1}^S q_s^* = 1 \quad (\text{C.2})$$

$$\sum_{s=1}^S q_s^* \cdot (f_{\text{regret}}^*(\cdot) - \tau^{(s)}(\cdot)) = 0 \quad (\text{C.3})$$

$$q_s^* \cdot (\mathbb{E}_{Q_{\mathbf{X}}}[(f_{\text{regret}}^*(\mathbf{X}) - \tau^{(s)}(\mathbf{X}))^2] - R^*) = 0 \quad \text{for } s \in [S] \quad (\text{C.4})$$

$$\mathbb{E}_{Q_{\mathbf{X}}}[(f_{\text{regret}}^*(\mathbf{X}) - \tau^{(s)}(\mathbf{X}))^2] - R^* \leq 0 \quad \text{for } s \in [S] \quad (\text{C.5})$$

$$q_s^* \geq 0 \quad \text{for } s \in [S] \quad (\text{C.6})$$

where Equation (C.3) is obtained by setting the functional derivative of the Lagrangian associated with Equation (7) with respect to $f(\cdot)$ to zero. These conditions indicate that $f_{\text{regret}}^*(\cdot)$ will be a convex combination of $\{\tau^{(s)}(\cdot)\}_{s=1}^S$, and $q_s^* = 0$ for any $s \in [S]$ such that $\|f_{\text{regret}}^*(\mathbf{X}) - \tau^{(s)}(\mathbf{X})\|_{Q_{\mathbf{X}},2}^2$ is strictly smaller than R^* . Since \mathcal{F} is convex and contains $\{\tau^{(s)}(\cdot)\}_{s=1}^S$, the optimal solution $(f_{\text{regret}}^*(\cdot), R^*)$ exists.

To solve the primal problem in Equation (7), we write out its Wolfe dual problem (Wolfe, 1961), which is given by:

$$\max_{R \in \mathbb{R}, f \in \mathcal{F}, \mathbf{q}} R + \sum_{s=1}^S q_s \cdot \left(\mathbb{E}_{Q_{\mathbf{X}}}[(f(\mathbf{X}) - \tau^{(s)}(\mathbf{X}))^2] - R \right), \quad (\text{C.7})$$

$$\text{subject to } \sum_{s=1}^S q_s = 1, \quad (\text{C.8})$$

$$\sum_{s=1}^S q_s \cdot (f(\cdot) - \tau^{(s)}(\cdot)) = 0 \quad (\text{C.9})$$

$$q_s \geq 0 \quad \text{for } s = 1, \dots, S. \quad (\text{C.10})$$

We will then show that this Wolfe dual problem is equivalent to a quadratic programming (QP) problem. First, rewrite the objective of the Wolfe dual problem as,

$$\begin{aligned} & \sum_{s=1}^S q_s \cdot \mathbb{E}_{Q_{\mathbf{X}}}[(f(\mathbf{X}) - \tau^{(s)}(\mathbf{X}))^2] \\ &= \sum_{s=1}^S q_s \cdot \mathbb{E}_{Q_{\mathbf{X}}}[f^2(\mathbf{X})] - 2\mathbb{E}_{Q_{\mathbf{X}}}\left[f(\mathbf{X}) \sum_{s=1}^S q_s \tau^{(s)}(\mathbf{X})\right] + \sum_{s=1}^S q_s \cdot \mathbb{E}_{Q_{\mathbf{X}}}[\tau^{(s)}(\mathbf{X})^2] \\ &= \sum_{s=1}^S q_s \cdot \mathbb{E}_{Q_{\mathbf{X}}}[\tau^{(s)}(\mathbf{X})^2] - \mathbb{E}_{Q_{\mathbf{X}}}\left[\left(\sum_{s=1}^S q_s \tau^{(s)}(\mathbf{X})\right)^2\right] \end{aligned}$$

where the second equality follows from Equations (C.8) and (C.9). Since the objective function in Equation (C.7) is independent of R for any feasible \mathbf{q} due to the constraint in Equation (C.8), we may choose R arbitrarily. Thus, the above Wolfe dual problem is equivalent to the following QP

problem:

$$\max_{\mathbf{q}} \sum_{s=1}^S q_s \cdot \mathbb{E}_{Q_{\mathbf{X}}} [\tau^{(s)}(\mathbf{X})^2] - \mathbb{E}_{Q_{\mathbf{X}}} \left[\left(\sum_{s=1}^S q_s \tau^{(s)}(\mathbf{X}) \right)^2 \right], \quad (\text{C.11})$$

$$\text{subject to } \sum_{s=1}^S q_s = 1, \quad (\text{C.12})$$

$$q_s \geq 0 \quad \text{for } s = 1, \dots, S, \quad (\text{C.13})$$

$$\text{with } f(\cdot) = \sum_{s=1}^S q_s \cdot \tau^{(s)}(\cdot), \quad (\text{C.14})$$

$$R = \sum_{s=1}^S q_s \cdot \mathbb{E}_{Q_{\mathbf{X}}} [(f(\mathbf{X}) - \tau^{(s)}(\mathbf{X}))^2]. \quad (\text{C.15})$$

The particular choice in Equation (C.15) will later ensure that solving the QP problem solves the primal problem. This QP optimization problem is concave because the objective can be written as $-(\mathbf{q}^\top \Gamma \mathbf{q} - \mathbf{q}^\top \mathbf{d})$ and Γ is positive semidefinite.

Next, we prove that the solution to the above QP problem is also the solution to the primal problem given in Equation (7). Suppose (\mathbf{q}^*, f^*, R^*) solves the QP problem. It suffices to show that (\mathbf{q}^*, f^*, R^*) satisfies the KKT conditions of the primal problem. Equations (C.2), (C.3) and (C.6) are directly satisfied by Equations (C.12), (C.14) and (C.13), respectively. We leverage the KKT conditions for the QP problem, which guarantees the existence of an unconstrained multiplier w^* and constrained multipliers $\{u_s^*\}_{s=1}^S$ such that:

$$2\mathbb{E} \left[\sum_{s=1}^S q_s^* \tau^{(s)}(\mathbf{X}) \cdot \tau^{(s')}(\mathbf{X}) \right] - \mathbb{E} [\tau^{(s')}(\mathbf{X})^2] + w^* - u_{s'}^* = 0 \quad \text{for } s' = 1, \dots, S, \quad (\text{C.16})$$

$$q_{s'}^* u_{s'}^* = 0 \quad \text{for } s' = 1, \dots, S, \quad (\text{C.17})$$

$$u_{s'}^* \geq 0 \quad \text{for } s' = 1, \dots, S. \quad (\text{C.18})$$

Using Equation (C.14), we rewrite Equation (C.16) as,

$$\left\| f^*(\mathbf{X}) - \tau^{(s')}(\mathbf{X}) \right\|_{Q_{\mathbf{X}},2}^2 - \mathbb{E} [f^*(\mathbf{X})^2] - w^* + u_{s'}^* = 0 \quad \text{for } s' = 1, \dots, S. \quad (\text{C.19})$$

In addition, after multiplying Equation (C.16) by $q_{s'}^*$ and summing it over s' , we use Equation (C.15) to obtain,

$$w^* = R^* - \mathbb{E} [f^*(\mathbf{X})^2]. \quad (\text{C.20})$$

Combining Equations (C.19) and (C.20), we obtain,

$$u_{s'}^* = R^* - \left\| f^*(\mathbf{X}) - \tau^{(s')}(\mathbf{X}) \right\|_{Q_{\mathbf{X}},2}^2, \quad s' = 1, \dots, S. \quad (\text{C.21})$$

Due to Equations (C.17) and (C.18), the primal KKT conditions, i.e., Equations (C.4) and (C.5) hold. Therefore, if (\mathbf{q}^*, f^*, R^*) solves the QP problem, then (f^*, R^*) solves the primal problem given in Equation (7). \square

C.3 Proof of Corollary 1

By definition, a polytope can be represented as the convex hull of a finite set of extreme points, corresponding to its vertices. Therefore, the uncertainty set $\mathcal{C}(Q_{\mathbf{X}}, \mathcal{H})$ can be expressed as a convex hull of N synthetic CATEs: $\{\mathbf{g}_1^\top \boldsymbol{\tau}, \dots, \mathbf{g}_N^\top \boldsymbol{\tau}\}$, where each CATE is a convex combination of the original S source sites CATEs. The result then follows directly from the proof of Theorem 1 by treating the N synthetic CATEs as the new set of source CATEs. \square

C.4 Proof of Theorem 2

Proof. According to the definition of \hat{f}_{regret} in Equation(12), we have that

$$\begin{aligned} \left(\hat{f}_{\text{regret}}(\cdot) - f_{\text{regret}}^*(\cdot)\right)^2 &= \left(\sum_{s=1}^S \hat{q}_s \cdot \hat{\tau}^{(s)}(\cdot) - \sum_{s=1}^S q_s^* \cdot \tau^{(s)}(\cdot)\right)^2 \\ &= \left(\sum_{s=1}^S \hat{q}_s \cdot \Delta^{(s)}(\cdot) - \sum_{s=1}^S (q_s^* - \hat{q}_s) \cdot \tau^{(s)}(\cdot)\right)^2 \end{aligned}$$

where $\Delta^{(s)}(\cdot) := \hat{\tau}^{(s)}(\cdot) - \tau^{(s)}(\cdot)$ denotes the estimation error of $\hat{\tau}^{(s)}$. It follows that

$$\left(\sum_{s=1}^S \hat{q}_s \cdot \Delta^{(s)}(\cdot) - \sum_{s=1}^S (q_s^* - \hat{q}_s) \cdot \tau^{(s)}(\cdot)\right)^2 \leq 2 \left(\left(\sum_{s=1}^S \hat{q}_s \cdot \Delta^{(s)}(\cdot)\right)^2 + \left(\sum_{s=1}^S (q_s^* - \hat{q}_s) \cdot \tau^{(s)}(\cdot)\right)^2 \right).$$

We then apply the Cauchy-Schwarz inequality to both terms on the right-hand side of the above inequality and establish that

$$\left(\sum_{s=1}^S \hat{q}_s \cdot \Delta^{(s)}(\cdot)\right)^2 \leq \sum_{s=1}^S \hat{q}_s^2 \sum_{s=1}^S \left(\Delta^{(s)}(\cdot)\right)^2 \leq \sum_{s=1}^S \left(\Delta^{(s)}(\cdot)\right)^2,$$

where the last inequality holds because $\{\hat{q}_s\}_{s=1}^S \in \Delta_{S-1}$. Furthermore:

$$\left(\sum_{s=1}^S (q_s^* - \hat{q}_s) \cdot \tau^{(s)}(\cdot)\right)^2 \leq \|\hat{\mathbf{q}} - \mathbf{q}^*\|_2^2 \sum_{s=1}^S \left(\tau^{(s)}(\cdot)\right)^2.$$

Then, we can quantify the error of $\|\hat{f}_{\text{regret}} - f_{\text{regret}}^*\|_{Q,2}$ as follows,

$$\begin{aligned} \|\hat{f}_{\text{regret}} - f_{\text{regret}}^*\|_{Q,2} &= \sqrt{\mathbb{E}_Q \left(\hat{f}_{\text{regret}}(\mathbf{X}) - f_{\text{regret}}^*(\mathbf{X}) \right)^2} \\ &\leq \sqrt{2 \left(\sum_{s=1}^S \mathbb{E}_Q [\Delta^{(s)}(\mathbf{X})^2] + \|\hat{\mathbf{q}} - \mathbf{q}^*\|_2^2 \sum_{s=1}^S \mathbb{E}_Q [\tau^{(s)}(\mathbf{X})^2] \right)} \quad (\text{C.22}) \\ &\leq \sqrt{2S \left(\delta_n^2 + \|\hat{\mathbf{q}} - \mathbf{q}^*\|_2^2 4M^2 \right)} \\ &\leq \sqrt{2S} (\delta_n + \|\hat{\mathbf{q}} - \mathbf{q}^*\|_2 2M), \end{aligned}$$

where the second inequality is due to Assumptions 4 and 5, and the last inequality holds because both M and δ_n are non-negative.

To upper bound the term $\|\hat{\mathbf{q}} - \mathbf{q}^*\|_2$, we will use the following lemma, which is adapted from Lemma 6 in Guo (2023) and Lemma 1 in Wang et al. (2023). For completeness, we include its proof in Appendix C.6.

Lemma 1 (Estimated weights for minimax-regret). Define the diameter of the simplex Δ_{S-1} as $\rho_{\Delta_{S-1}} = \max_{\mathbf{q}, \mathbf{q}' \in \Delta_{S-1}} \|\mathbf{q} - \mathbf{q}'\|_2$. Recall the definitions of $\mathbf{q}^* = \arg \min_{\mathbf{q} \in \Delta_{S-1}} \mathbf{q}^\top \Gamma \mathbf{q} - \mathbf{q}^\top \mathbf{d}$ in Equation (9) and $\hat{\mathbf{q}} = \arg \min_{\mathbf{q} \in \Delta_{S-1}} \mathbf{q}^\top \hat{\Gamma} \mathbf{q} - \mathbf{q}^\top \hat{\mathbf{d}}$ in Equation (12). If $\lambda_{\min}(\Gamma) > 0$, then

$$\|\hat{\mathbf{q}} - \mathbf{q}^*\|_2 \leq \frac{S(\|\hat{\Gamma} - \Gamma\|_\infty + \frac{1}{2}\|\hat{\mathbf{d}} - \mathbf{d}\|_\infty)}{\lambda_{\min}(\Gamma)} \wedge \rho_{\Delta_{S-1}},$$

where $\|\hat{\Gamma} - \Gamma\|_\infty$ is the element-wise maximum norm of a matrix, and $\|\hat{\mathbf{d}} - \mathbf{d}\|_\infty$ is the ℓ_∞ norm of a vector.

By Lemma 1, we only need to bound the terms $\|\hat{\Gamma} - \Gamma\|_\infty$ and $\|\hat{\mathbf{d}} - \mathbf{d}\|_\infty$. For fixed $k, l \in [S]$, we decompose the error of $\hat{\Gamma}$ into two parts as follows:

$$\begin{aligned} & (\hat{\Gamma} - \Gamma)_{k,l} \\ &= \frac{1}{n_Q} \sum_{i=1}^{n_Q} \hat{\tau}^{(k)}(\mathbf{X}_i) \hat{\tau}^{(l)}(\mathbf{X}_i) - \mathbb{E}_{Q, \mathbf{X}} \left[\tau^{(k)}(\mathbf{X}) \tau^{(l)}(\mathbf{X}) \right] \\ &= \underbrace{\frac{1}{n_Q} \sum_{i=1}^{n_Q} \left(\hat{\tau}^{(k)}(\mathbf{X}_i) \hat{\tau}^{(l)}(\mathbf{X}_i) - \tau^{(k)}(\mathbf{X}_i) \tau^{(l)}(\mathbf{X}_i) \right)}_{(\text{I})_{k,l}} + \underbrace{\frac{1}{n_Q} \sum_{i=1}^{n_Q} \left(\tau^{(k)}(\mathbf{X}_i) \tau^{(l)}(\mathbf{X}_i) - \mathbb{E}_{Q, \mathbf{X}} \left[\tau^{(k)}(\mathbf{X}) \tau^{(l)}(\mathbf{X}) \right] \right)}_{(\text{II})_{k,l}}. \end{aligned}$$

We will upper-bound each term. For the term $(\text{I})_{k,l}$, which represents the estimation error of $\tau^{(k)}$ and $\tau^{(l)}$, we further decompose it into the following components,

$$\begin{aligned} |(\text{I})_{k,l}| &= \left| \frac{1}{n_Q} \sum_{i=1}^{n_Q} \tau^{(k)}(\mathbf{X}_i) \Delta^{(l)}(\mathbf{X}_i) + \frac{1}{n_Q} \sum_{i=1}^{n_Q} \tau^{(l)}(\mathbf{X}_i) \Delta^{(k)}(\mathbf{X}_i) + \frac{1}{n_Q} \sum_{i=1}^{n_Q} \Delta^{(k)}(\mathbf{X}_i) \Delta^{(l)}(\mathbf{X}_i) \right| \\ &\leq \left| \frac{1}{n_Q} \sum_{i=1}^{n_Q} \tau^{(k)}(\mathbf{X}_i) \Delta^{(l)}(\mathbf{X}_i) \right| + \left| \frac{1}{n_Q} \sum_{i=1}^{n_Q} \tau^{(l)}(\mathbf{X}_i) \Delta^{(k)}(\mathbf{X}_i) \right| + \left| \frac{1}{n_Q} \sum_{i=1}^{n_Q} \Delta^{(k)}(\mathbf{X}_i) \Delta^{(l)}(\mathbf{X}_i) \right| \\ &\leq 2M \sqrt{\frac{1}{n_Q} \sum_{i=1}^{n_Q} (\Delta^{(l)}(\mathbf{X}_i))^2} + 2M \sqrt{\frac{1}{n_Q} \sum_{i=1}^{n_Q} (\Delta^{(k)}(\mathbf{X}_i))^2} \\ &\quad + \sqrt{\frac{1}{n_Q} \sum_{i=1}^{n_Q} (\Delta^{(l)}(\mathbf{X}_i))^2} \sqrt{\frac{1}{n_Q} \sum_{i=1}^{n_Q} (\Delta^{(k)}(\mathbf{X}_i))^2}. \end{aligned} \tag{C.23}$$

where the first inequality is due to the triangle inequality, and the second inequality is derived from the Cauchy-Schwarz inequality. Next, we apply Markov's inequality to further upper-bound the terms in the above inequality. For any $t > 1$, the following inequality holds due to Assumption 5:

$$\mathbb{P} \left\{ \frac{1}{n_Q} \sum_{i=1}^{n_Q} (\Delta^{(l)}(\mathbf{X}_i))^2 \geq tS\delta_n^2 \right\} \leq \frac{\mathbb{E}_Q [\Delta^{(l)}(\mathbf{X})^2]}{tS\delta_n^2} \leq \frac{1}{tS}.$$

Then, by union bound, we have

$$\mathbb{P}\left(\max_{l \in [S]} \left\{ \frac{1}{n_Q} \sum_{i=1}^{n_Q} \left(\Delta^{(l)}(\mathbf{X}_i) \right)^2 \right\} \leq tS\delta_n^2\right) \geq 1 - S \cdot \frac{1}{tS} = 1 - \frac{1}{t}.$$

Therefore, with probability at least $1 - \frac{1}{t}$, we have,

$$\max_{k,l} |(\text{I})_{k,l}| \leq 4M\sqrt{tS} \cdot \delta_n + tS \cdot \delta_n^2. \quad (\text{C.24})$$

Next, for the term $(\text{II})_{k,l}$, we apply Chebyshev's inequality to upper-bound the term. For any $c > 0$,

$$\begin{aligned} \mathbb{P}\left(\left| \frac{1}{n_Q} \sum_{i=1}^{n_Q} \tau^{(k)}(\mathbf{X}_i)\tau^{(l)}(\mathbf{X}_i) - \mathbb{E}_{Q_{\mathbf{X}}}\left[\tau^{(k)}(\mathbf{X})\tau^{(l)}(\mathbf{X})\right] \right| \geq c\right) &\leq \frac{\text{Var}\left[\frac{1}{n_Q} \sum_{i=1}^{n_Q} \tau^{(k)}(\mathbf{X}_i)\tau^{(l)}(\mathbf{X}_i)\right]}{c^2} \\ &\leq \frac{\mathbb{E}\left[\left(\tau^{(k)}(\mathbf{X}_i)\tau^{(l)}(\mathbf{X}_i)\right)^2\right]}{n_Q c^2} \leq \frac{16M^4}{n_Q c^2}. \end{aligned} \quad (\text{C.25})$$

For $t > 1$, we take $c = 4M^2 tS / \sqrt{n_Q}$, then the above inequality becomes:

$$\mathbb{P}\left(\left| \frac{1}{n_Q} \sum_{i=1}^{n_Q} \tau^{(k)}(\mathbf{X}_i)\tau^{(l)}(\mathbf{X}_i) - \mathbb{E}_{Q_{\mathbf{X}}}\left[\tau^{(k)}(\mathbf{X})\tau^{(l)}(\mathbf{X})\right] \right| \geq 4tS \frac{M^2}{\sqrt{n_Q}}\right) \leq \frac{1}{t^2 S^2}.$$

Then, by union bound, with probability at least $1 - \frac{1}{t^2}$,

$$\max_{k,l} |(\text{II})_{k,l}| \leq \frac{4tSM^2}{\sqrt{n_Q}}. \quad (\text{C.26})$$

Combining the inequalities in Equations (C.24) and (C.26), we establish that, with probability at least $1 - \frac{1}{t} - \frac{1}{t^2}$,

$$\|\hat{\Gamma} - \Gamma\|_{\infty} \leq \left(\max_{k,l} |(\text{I})_{k,l}| + \max_{k,l} |(\text{II})_{k,l}| \right) \leq tS \left(\frac{4M\delta_n}{\sqrt{tS}} + \delta_n^2 + \frac{4M^2}{\sqrt{n_Q}} \right).$$

In the meantime, the following inequality also holds:

$$\|\hat{\mathbf{d}} - \mathbf{d}\|_{\infty} = \max_{s \in [S]} \left| \hat{\Gamma}_{s,s} - \Gamma_{s,s} \right| \leq tS \left(\frac{4M\delta_n}{\sqrt{tS}} + \delta_n^2 + \frac{4M^2}{\sqrt{n_Q}} \right).$$

Combining the above inequalities with Lemma 1, we obtain that, with probability at least $1 - \frac{1}{t} - \frac{1}{t^2}$,

$$\left\| \hat{f}_{\text{regret}} - f_{\text{regret}}^* \right\|_{Q,2} \leq \sqrt{2S} \left(\delta_n + \left(\frac{1.5tS^2 \left(\frac{4M\delta_n}{\sqrt{tS}} + \delta_n^2 + \frac{4M^2}{\sqrt{n_Q}} \right)}{\lambda_{\min}(\Gamma)} \wedge \rho_{\mathcal{H}} \right) 2M \right).$$

□

C.5 Proof of Proposition 2

We generalize the proof of Theorem 1 of Wang et al. (2023), which considers a special case of $f_{\text{base}} = 0$.

Proof. For a target distribution $Q \in \mathcal{C}(Q_{\mathbf{X}}, \mathcal{H})$, define the population relative-risk function for the function $f(\cdot)$ as:

$$\begin{aligned} R_Q(f) &:= \mathbb{E}_Q[(Y(1) - Y(0) - f(\mathbf{X}))^2 - (Y(1) - Y(0) - f_{\text{base}}(\mathbf{X}))^2] \\ &= \mathbb{E}_Q[-2(Y(1) - Y(0))(f(\mathbf{X}) - f_{\text{base}}(\mathbf{X})) + f(\mathbf{X})^2 - f_{\text{base}}(\mathbf{X})^2]. \end{aligned}$$

By the definition of Q , the target CATE is a weighted average of source CATEs, characterized by $\tau_Q(\cdot) = \sum_{s=1}^S q_s \cdot \tau^{(s)}(\cdot)$ for $\mathbf{q} \in \mathcal{H}$.

Therefore, Equation (15) can be written as:

$$\begin{aligned} f_{\text{rel}}^*(\cdot; f_{\text{base}}) &= \arg \min_{f \in \mathcal{F}} \max_{Q \in \mathcal{C}(Q_{\mathbf{X}}, \mathcal{H})} R_Q(f) \\ &= \arg \min_{f \in \mathcal{F}} \max_{\mathbf{q} \in \mathcal{H}} \sum_{s=1}^S q_s \cdot \mathbb{E}_{Q_{\mathbf{X}}} \left[-2\tau^{(s)}(\mathbf{X})(f(\mathbf{X}) - f_{\text{base}}(\mathbf{X})) + f(\mathbf{X})^2 - f_{\text{base}}(\mathbf{X})^2 \right]. \end{aligned} \quad (\text{C.27})$$

Suppose that we can swap the order of min and max, which will be justified later. Then, the objective can be rewritten as,

$$\arg \max_{\mathbf{q} \in \mathcal{H}} \min_{f \in \mathcal{F}} \sum_{s=1}^S q_s \cdot \mathbb{E}_{Q_{\mathbf{X}}} \left[-2\tau^{(s)}(\mathbf{X})(f(\mathbf{X}) - f_{\text{base}}(\mathbf{X})) + f(\mathbf{X})^2 - f_{\text{base}}(\mathbf{X})^2 \right]. \quad (\text{C.28})$$

For any given $\mathbf{q} \in \mathcal{H}$, the solution to the inner minimization is given by,

$$\begin{aligned} f^{\mathbf{q}}(\cdot) &= \arg \min_{f \in \mathcal{F}} \mathbb{E}_{Q_{\mathbf{X}}} \left[-2 \sum_{s=1}^S q_s \cdot \tau^{(s)}(\mathbf{X}) f(\mathbf{X}) + f(\mathbf{X})^2 \right] \\ &= \arg \min_{f \in \mathcal{F}} \mathbb{E}_{Q_{\mathbf{X}}} \left[f(\mathbf{X}) - \sum_{s=1}^S q_s \cdot \tau^{(s)}(\mathbf{X}) \right]^2 \\ &= \sum_{s=1}^S q_s \cdot \tau^{(s)}(\cdot), \end{aligned} \quad (\text{C.29})$$

where the second equality follows because the function class \mathcal{F} contains all the $\{\tau^{(s)}(\cdot)\}_{s=1}^S$ and is convex. Thus, the solution to the optimization problem in Equation (C.28) is given by:

$$\mathbf{q}^* = \arg \min_{\mathbf{q} \in \mathcal{H}} \mathbb{E}_{Q_{\mathbf{X}}} \left[\sum_{s=1}^S q_s \cdot \tau^{(s)}(\mathbf{X}) - f_{\text{base}}(\mathbf{X}) \right]^2$$

and

$$f_{\text{swap}}^*(\cdot) = \sum_{s=1}^S q_s^* \cdot \tau^{(s)}(\cdot). \quad (\text{C.30})$$

Next, we provide a justification for interchanging max and min by showing that $f_{\text{swap}}^*(\cdot)$ is also the solution to the original objective given in Equation (C.27). For any $t \in [0, 1]$ and $\mathbf{q} \in \mathcal{H}$, we

use the fact that $\mathbf{q}^* + t(\mathbf{q} - \mathbf{q}^*) \in \mathcal{H}$ and by the definition of \mathbf{q}^* , we have

$$\mathbb{E}_{Q_{\mathbf{X}}} \left[\sum_{s=1}^S (q_s^* + t(q_s - q_s^*)) \cdot \tau^{(s)}(\mathbf{X}) - f_{\text{base}}(\mathbf{X}) \right]^2 \geq \mathbb{E}_{Q_{\mathbf{X}}} \left[\sum_{s=1}^S q_s^* \cdot \tau^{(s)}(\mathbf{X}) - f_{\text{base}}(\mathbf{X}) \right]^2.$$

The above inequality further implies

$$t^2 \cdot \mathbb{E}_{Q_{\mathbf{X}}} \left[\sum_{s=1}^S (q_s - q_s^*) \tau^{(s)}(\mathbf{X}) \right]^2 + 2t \cdot \mathbb{E}_{Q_{\mathbf{X}}} \left[\left(\sum_{s=1}^S q_s^* \cdot \tau^{(s)}(\mathbf{X}) - f_{\text{base}}(\mathbf{X}) \right) \left(\sum_{s=1}^S (q_s - q_s^*) \tau^{(s)}(\mathbf{X}) \right) \right] \geq 0$$

for all $t \in [0, 1]$. By taking $t \rightarrow 0+$, we have,

$$\mathbb{E}_{Q_{\mathbf{X}}} \left[\left(\sum_{s=1}^S q_s^* \cdot \tau^{(s)}(\mathbf{X}) - f_{\text{base}}(\mathbf{X}) \right) \left(\sum_{s=1}^S (q_s - q_s^*) \tau^{(s)}(\mathbf{X}) \right) \right] \geq 0,$$

which is equivalent to, for any $\mathbf{q} \in \mathcal{H}$,

$$\begin{aligned} & \mathbb{E}_{Q_{\mathbf{X}}} \left[\left(\sum_{s=1}^S q_s^* \cdot \tau^{(s)}(\mathbf{X}) - f_{\text{base}}(\mathbf{X}) \right) \left(\sum_{s=1}^S q_s \cdot \tau^{(s)}(\mathbf{X}) \right) \right] \\ & \geq \mathbb{E}_{Q_{\mathbf{X}}} \left[\sum_{s=1}^S q_s^* \cdot \tau^{(s)}(\mathbf{X}) \right]^2 - \mathbb{E}_{Q_{\mathbf{X}}} \left[\sum_{s=1}^S q_s^* \tau^{(s)}(\mathbf{X}) \cdot f_{\text{base}}(\mathbf{X}) \right]. \end{aligned} \quad (\text{C.31})$$

Given the original objective in Equation (C.27), we have the following inequality,

$$\begin{aligned} & \min_{f \in \mathcal{F}} \max_{\mathbf{q} \in \mathcal{H}} \mathbb{E}_{Q_{\mathbf{X}}} \left[-2 \sum_{s=1}^S q_s \cdot \tau^{(s)}(\mathbf{X}) (f(\mathbf{X}) - f_{\text{base}}(\mathbf{X})) + f(\mathbf{X})^2 - f_{\text{base}}(\mathbf{X})^2 \right] \\ & \leq \max_{\mathbf{q} \in \mathcal{H}} \mathbb{E}_{Q_{\mathbf{X}}} \left[-2 \sum_{s=1}^S q_s \cdot \tau^{(s)}(\mathbf{X}) (f_{\text{swap}}^*(\mathbf{X}) - f_{\text{base}}(\mathbf{X})) + f_{\text{swap}}^*(\mathbf{X})^2 - f_{\text{base}}(\mathbf{X})^2 \right] \\ & = \max_{\mathbf{q} \in \mathcal{H}} \mathbb{E}_{Q_{\mathbf{X}}} \left[-2 \left(\sum_{s=1}^S q_s \cdot \tau^{(s)}(\mathbf{X}) \right) \left(\sum_{s=1}^S q_s^* \cdot \tau^{(s)}(\mathbf{X}) - f_{\text{base}}(\mathbf{X}) \right) + \left(\sum_{s=1}^S q_s^* \cdot \tau^{(s)}(\mathbf{X}) \right)^2 - f_{\text{base}}(\mathbf{X})^2 \right] \\ & \leq - \mathbb{E}_{Q_{\mathbf{X}}} \left[\sum_{s=1}^S q_s^* \cdot \tau^{(s)}(\mathbf{X}) - f_{\text{base}}(\mathbf{X}) \right]^2, \end{aligned} \quad (\text{C.32})$$

where the first inequality follows because $f_{\text{swap}}^* \in \mathcal{F}$, and the last inequality holds due to Equation (C.31). Moreover, since $\mathbf{q}^* \in \mathcal{H}$, we have,

$$\begin{aligned} & \min_{f \in \mathcal{F}} \max_{\mathbf{q} \in \mathcal{H}} \mathbb{E}_{Q_{\mathbf{X}}} \left[-2 \sum_{s=1}^S q_s \cdot \tau^{(s)}(\mathbf{X}) (f(\mathbf{X}) - f_{\text{base}}(\mathbf{X})) + f(\mathbf{X})^2 - f_{\text{base}}(\mathbf{X})^2 \right] \\ & \geq \min_{f \in \mathcal{F}} \mathbb{E}_{Q_{\mathbf{X}}} \left[-2 \sum_{s=1}^S q_s^* \cdot \tau^{(s)}(\mathbf{X}) (f(\mathbf{X}) - f_{\text{base}}(\mathbf{X})) + f(\mathbf{X})^2 - f_{\text{base}}(\mathbf{X})^2 \right] \\ & \geq - \mathbb{E}_{Q_{\mathbf{X}}} \left[\sum_{s=1}^S q_s^* \cdot \tau^{(s)}(\mathbf{X}) - f_{\text{base}}(\mathbf{X}) \right]^2, \end{aligned} \quad (\text{C.33})$$

where the last inequality follows from the fact that by definition of $f^{\mathbf{q}}(\cdot)$ in Equation (C.29), the minimizer of the right hand side of the above inequality is exactly $f_{\text{swap}}^*(\cdot)$ defined in Equation (C.30).

Combining Equations (C.32) and (C.33), we have shown that the original optimization problem achieves the optimal value $\mathbb{E}_{Q_{\mathbf{X}}} \left[\sum_{s=1}^S q_s^* \cdot \tau^{(s)}(\mathbf{X}) - f_{\text{base}}(\mathbf{X}) \right]^2$. Since $f_{\text{swap}}^*(\cdot) \in \mathcal{F}$ and $\mathbf{q}^* \in \mathcal{H}$, we have established that $f_{\text{swap}}^*(\cdot)$ is the optimizer to the original objective. \square

C.6 Proof of Lemma 1

Proof. By the definition of \mathbf{q}^* , for any $t \in (0, 1)$, we have

$$(\mathbf{q}^*)^\top \Gamma \mathbf{q}^* - (\mathbf{q}^*)^\top \mathbf{d} \leq [\mathbf{q}^* + t(\hat{\mathbf{q}} - \mathbf{q}^*)]^\top \Gamma [\mathbf{q}^* + t(\hat{\mathbf{q}} - \mathbf{q}^*)] - (\mathbf{q}^* + t(\hat{\mathbf{q}} - \mathbf{q}^*))^\top \mathbf{d}.$$

By taking $t \rightarrow 0+$, we have

$$2(\mathbf{q}^*)^\top \Gamma (\hat{\mathbf{q}} - \mathbf{q}^*) - (\hat{\mathbf{q}} - \mathbf{q}^*)^\top \mathbf{d} \geq 0. \quad (\text{C.34})$$

Similarly, by the definition of $\hat{\mathbf{q}}$, for any $t \in (0, 1)$, we have

$$(\hat{\mathbf{q}})^\top \hat{\Gamma} \hat{\mathbf{q}} - (\hat{\mathbf{q}})^\top \hat{\mathbf{d}} \leq [\hat{\mathbf{q}} + t(\mathbf{q}^* - \hat{\mathbf{q}})]^\top \hat{\Gamma} [\hat{\mathbf{q}} + t(\mathbf{q}^* - \hat{\mathbf{q}})] - (\hat{\mathbf{q}} + t(\mathbf{q}^* - \hat{\mathbf{q}}))^\top \hat{\mathbf{d}}$$

and therefore,

$$t^2 (\mathbf{q}^* - \hat{\mathbf{q}})^\top \hat{\Gamma} (\mathbf{q}^* - \hat{\mathbf{q}}) + 2t (\mathbf{q}^* - \hat{\mathbf{q}})^\top \hat{\Gamma} \hat{\mathbf{q}} - t (\mathbf{q}^* - \hat{\mathbf{q}})^\top \hat{\mathbf{d}} \geq 0.$$

Dividing by $t > 0$ results in the following inequality:

$$2(\mathbf{q}^*)^\top \hat{\Gamma} (\mathbf{q}^* - \hat{\mathbf{q}}) + (t - 2) (\mathbf{q}^* - \hat{\mathbf{q}})^\top \hat{\Gamma} (\mathbf{q}^* - \hat{\mathbf{q}}) - (\mathbf{q}^* - \hat{\mathbf{q}})^\top \hat{\mathbf{d}} \geq 0.$$

Since $2 - t > 0$, we have

$$(\mathbf{q}^* - \hat{\mathbf{q}})^\top \hat{\Gamma} (\mathbf{q}^* - \hat{\mathbf{q}}) \leq \frac{1}{2-t} \left[2(\mathbf{q}^*)^\top \hat{\Gamma} (\mathbf{q}^* - \hat{\mathbf{q}}) - (\mathbf{q}^* - \hat{\mathbf{q}})^\top \hat{\mathbf{d}} \right]. \quad (\text{C.35})$$

Furthermore, we have,

$$\begin{aligned} & 2(\mathbf{q}^*)^\top \hat{\Gamma} (\mathbf{q}^* - \hat{\mathbf{q}}) - (\mathbf{q}^* - \hat{\mathbf{q}})^\top \hat{\mathbf{d}} \\ &= 2(\mathbf{q}^*)^\top (\hat{\Gamma} - \Gamma) (\mathbf{q}^* - \hat{\mathbf{q}}) + 2(\mathbf{q}^*)^\top \Gamma (\mathbf{q}^* - \hat{\mathbf{q}}) - (\mathbf{q}^* - \hat{\mathbf{q}})^\top \mathbf{d} - (\mathbf{q}^* - \hat{\mathbf{q}})^\top (\hat{\mathbf{d}} - \mathbf{d}) \\ &\leq 2(\mathbf{q}^*)^\top (\hat{\Gamma} - \Gamma) (\mathbf{q}^* - \hat{\mathbf{q}}) - (\mathbf{q}^* - \hat{\mathbf{q}})^\top (\hat{\mathbf{d}} - \mathbf{d}). \end{aligned}$$

where the inequality follows from Equation (C.34). Combining this with Equation (C.35), we obtain that

$$(\mathbf{q}^* - \hat{\mathbf{q}})^\top \hat{\Gamma} (\mathbf{q}^* - \hat{\mathbf{q}}) \leq \frac{1}{2-t} \left[2(\mathbf{q}^*)^\top (\hat{\Gamma} - \Gamma) (\mathbf{q}^* - \hat{\mathbf{q}}) - (\mathbf{q}^* - \hat{\mathbf{q}})^\top (\hat{\mathbf{d}} - \mathbf{d}) \right]. \quad (\text{C.36})$$

Since the $\hat{\mathbf{q}}$ and \mathbf{q}^* are symmetric, we switch the roles of $\{\hat{\Gamma}, \hat{\mathbf{d}}, \hat{\mathbf{q}}\}, \{\Gamma, \mathbf{d}, \mathbf{q}^*\}$ and establish:

$$\begin{aligned} (\mathbf{q}^* - \hat{\mathbf{q}})^\top \Gamma (\mathbf{q}^* - \hat{\mathbf{q}}) &\leq \frac{1}{2-t} \left[2(\hat{\mathbf{q}})^\top (\Gamma - \hat{\Gamma}) (\hat{\mathbf{q}} - \mathbf{q}^*) - (\hat{\mathbf{q}} - \mathbf{q}^*)^\top (\mathbf{d} - \hat{\mathbf{d}}) \right] \\ &\leq \frac{1}{2-t} \left[2\|\hat{\mathbf{q}}\|_2 \|\hat{\Gamma} - \Gamma\|_2 \|\mathbf{q}^* - \hat{\mathbf{q}}\|_2 + \|\mathbf{q}^* - \hat{\mathbf{q}}\|_2 \|\mathbf{d} - \hat{\mathbf{d}}\|_2 \right]. \end{aligned} \quad (\text{C.37})$$

Since $\lambda_{\min}(\Gamma) \|\mathbf{q}^* - \hat{\mathbf{q}}\|_2^2 \leq (\mathbf{q}^* - \hat{\mathbf{q}})^\top \Gamma (\mathbf{q}^* - \hat{\mathbf{q}})$, we obtain,

$$\lambda_{\min}(\Gamma) \|\mathbf{q}^* - \hat{\mathbf{q}}\|_2^2 \leq \frac{1}{2-t} \left[2\|\hat{\mathbf{q}}\|_2 \|\hat{\Gamma} - \Gamma\|_2 \|\mathbf{q}^* - \hat{\mathbf{q}}\|_2 + \|\mathbf{q}^* - \hat{\mathbf{q}}\|_2 \|\mathbf{d} - \hat{\mathbf{d}}\|_2 \right],$$

where $\|\hat{\Gamma} - \Gamma\|_2$ denotes the spectral norm of the matrix, $\hat{\Gamma} - \Gamma$.

Finally, if $\lambda_{\min}(\Gamma) > 0$, we can establish the result by letting $t \rightarrow 0+$:

$$\|\mathbf{q}^* - \hat{\mathbf{q}}\|_2 \leq \frac{1}{\lambda_{\min}(\Gamma)} \left[\|\hat{\Gamma} - \Gamma\|_2 + \frac{1}{2} \|\mathbf{d} - \hat{\mathbf{d}}\|_2 \right] \leq \frac{S(\|\hat{\Gamma} - \Gamma\|_\infty + \frac{1}{2} \|\mathbf{d} - \hat{\mathbf{d}}\|_\infty)}{\lambda_{\min}(\Gamma)},$$

where the last inequality is due to the fact that $\|\hat{\Gamma} - \Gamma\|_2 \leq \|\hat{\Gamma} - \Gamma\|_F \leq S\|\hat{\Gamma} - \Gamma\|_\infty$. \square

D Additional Tables and Figures

D.1 Additional Simulation Results

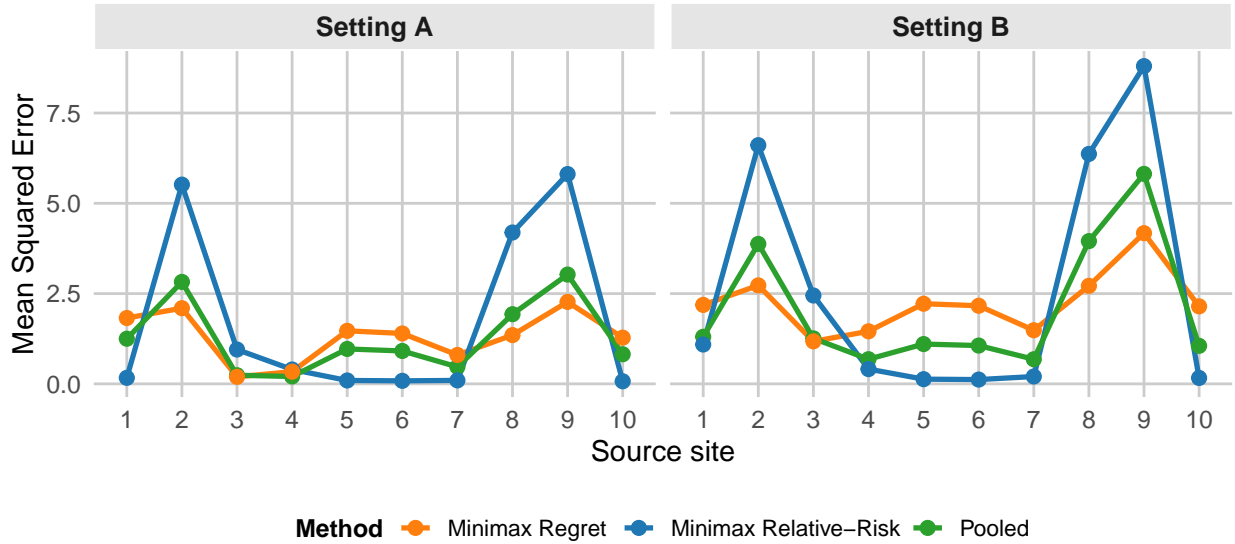


Figure D.1: Average MSE of multisite CATE estimates from three methods across 1,000 simulations, evaluated over different source sites, using **X-learner** as the site-specific CATE estimation method.

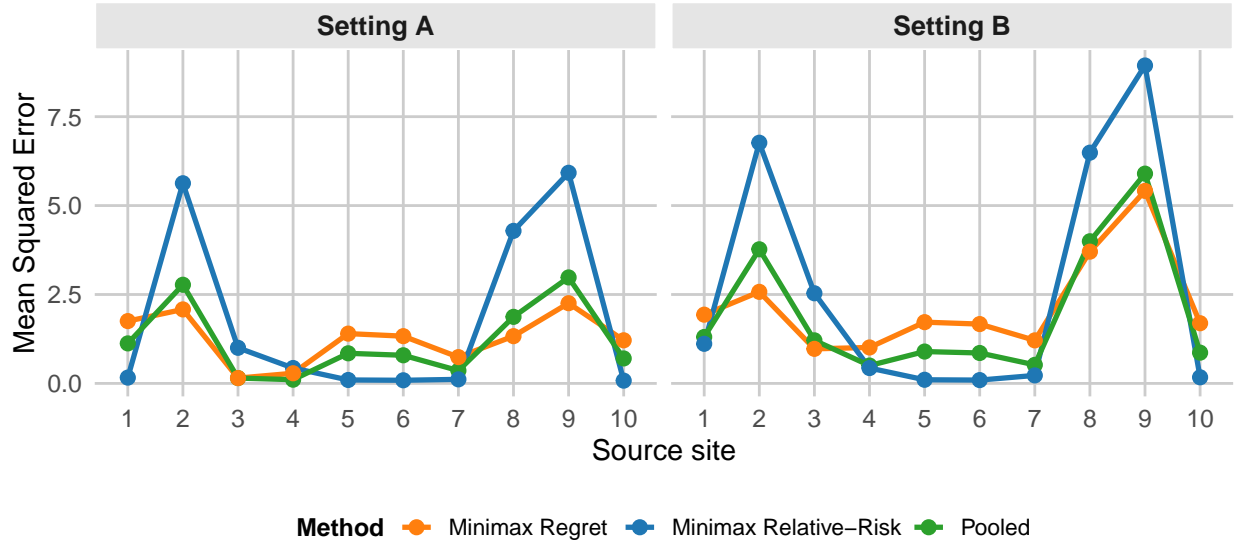


Figure D.2: Average MSE of multisite CATE estimates from three methods across 1,000 simulations, evaluated over different source sites, using **causal forest** as the site-specific CATE estimation method.

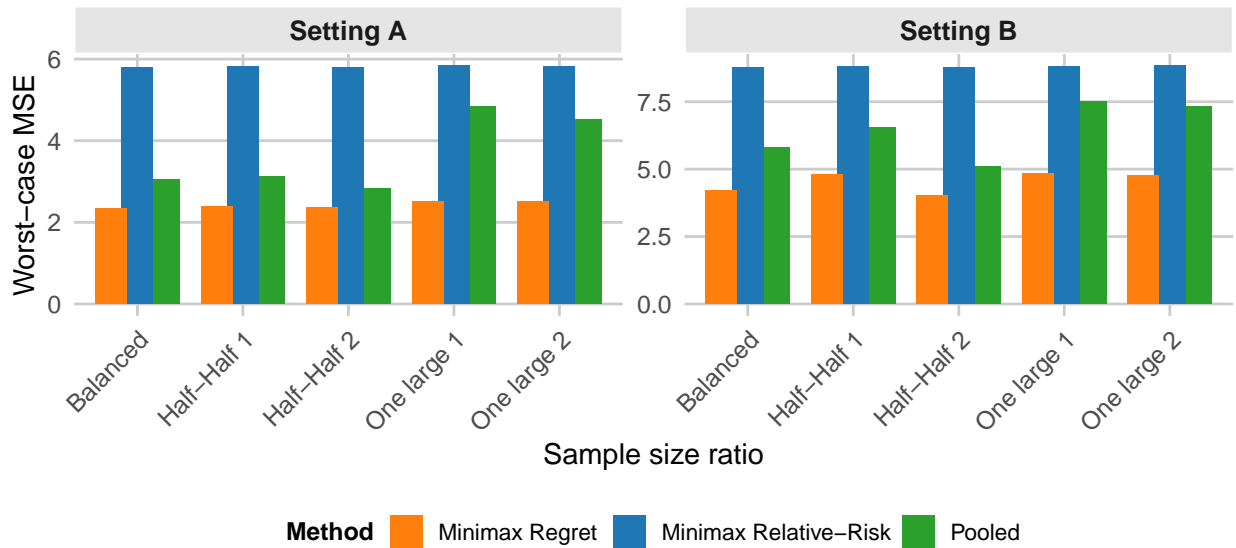


Figure D.3: Worst-case MSE averaged across 1,000 iterations under varying sample size ratios: (1) **Balanced**: all sites have equal sample sizes, (2) **Half-and-Half**: half of the sites have three times the sample size of the others, and (3) **One Large**: one site has a sample size 10 times larger than the others. For scenarios (2) and (3), we evaluate two configurations, each with a different subset of large sites. We use **X-learner** for site-specific CATE estimation.

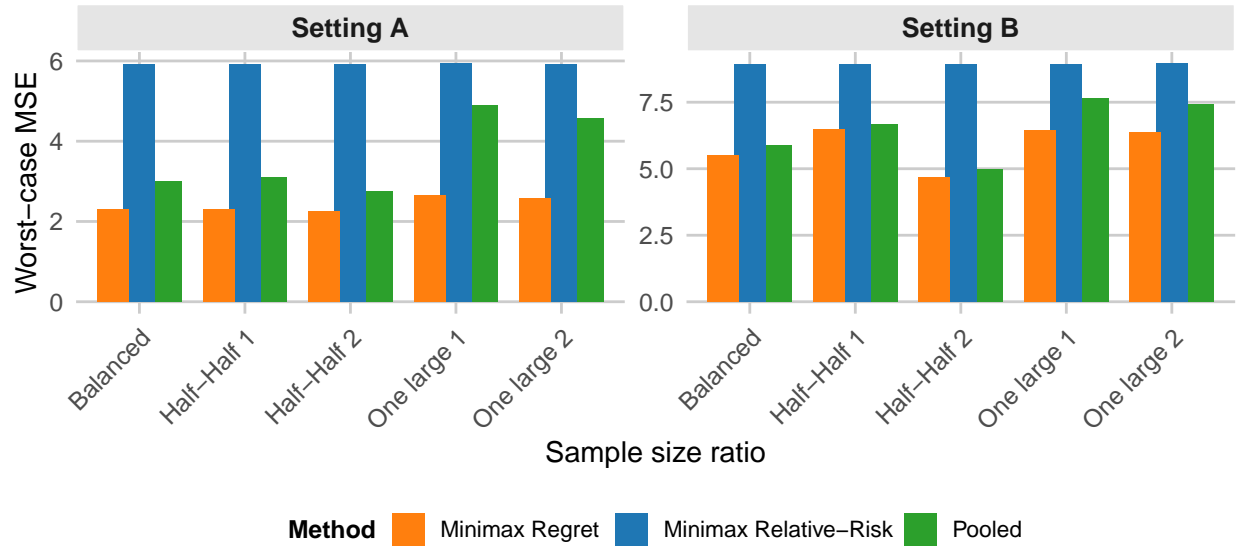


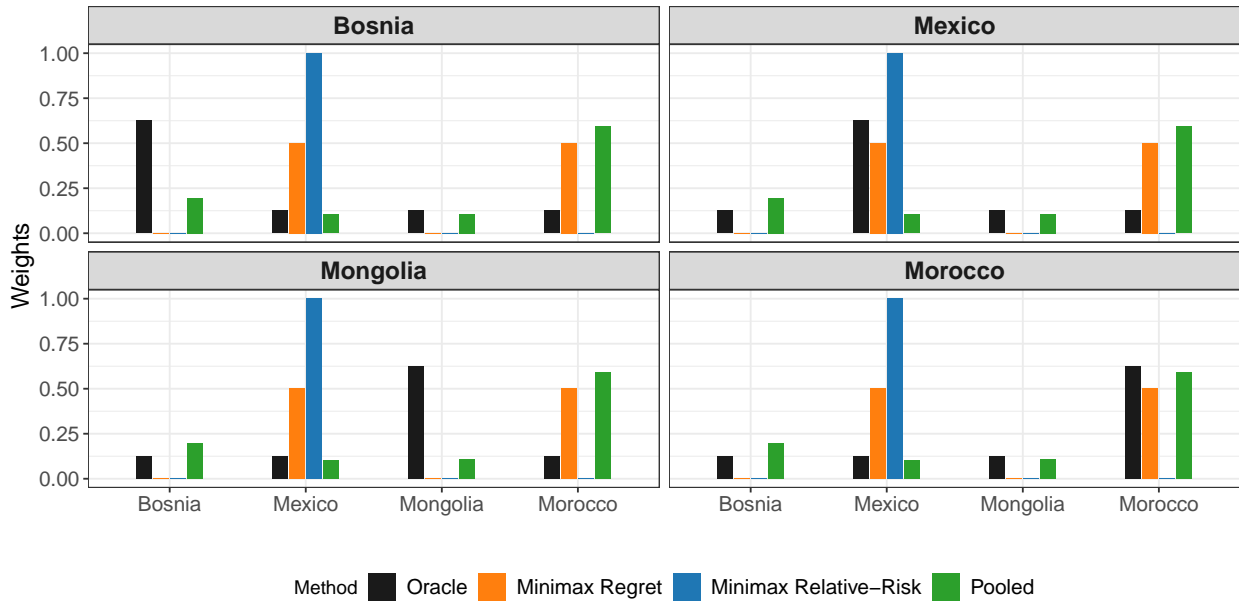
Figure D.4: Worst-case MSE averaged across 1,000 iterations under varying sample size ratios: (1) **Balanced**: all sites have equal sample sizes, (2) **Half-and-Half**: half of the sites have three times the sample size of the others, and (3) **One Large**: one site has a sample size 10 times larger than the others. For scenarios (2) and (3), we evaluate two configurations, each with a different subset of large sites. We use **causal forest** for site-specific CATE estimation.

D.2 Additional Empirical Application Results

| Study | Bosnia & Herzegovina | Mexico | Mongolia | Morocco |
|-------------------------------|--|---|---|--------------------------------------|
| | Augsburg et al. (2015) | Angelucci et al. (2015) | Attanasio et al. (2015) | Crépon et al. (2015) |
| Treatment | Provide loans to marginally rejected borrowers | Open branches, promote loans | Open branches, target likely borrowers | Open branches |
| Treatment Prop. | 0.55 | 0.37 | 0.73 | 0.49 |
| Randomization Level | Individual | Community | Community | Community |
| Urban/Rural | Both | Both | Rural | Rural |
| Target Women? | No | Yes | Yes | No |
| MFI already operates locally? | Yes | No | No | No |
| Microloan Type | Individual | Group | Both | Group |
| Collateralized | Yes | No | Yes | No |
| Other competing MFI's | Yes | Yes | Yes | No |
| Avg. interest rate | 22% APR | 100% APR | 24\$ APR | 13.5% APR |
| Sampling Frame | Marginal applicants | Women between 18-60 who own businesses (or wish to start one) | Women who registered interest in loans and met eligibility criteria | Random sample with likely borrowers |
| Study Duration | 14 months | 16 months | 19 months | 24 months |
| Demographic Covariates | | | | |
| Female | 0.41 | 1.00 | 1.00 | 0.15 |
| Age | 37.78 | 37.37 | 39.96 | 47.50 |
| Baseline Profit | 3321.91 | -16.51 | 19.98 | 341.39 |
| Baseline Expenditures | 1167.80 | 1104.16 | 53.00 | 470.88 |
| Baseline Loan Amount | 4049.07 | 276.63 | 0.00 | 234.38 |
| Existing Business | 0.62 | 0.48 | 0.60 | 0.12 |

Table D.1: Summary of the different sites. Akin to [Meager \(2019\)](#), we emphasize differences across the experiments in the sampling frame, as well as treatment implementation.

(a) Scenario 3



(b) Scenario 4

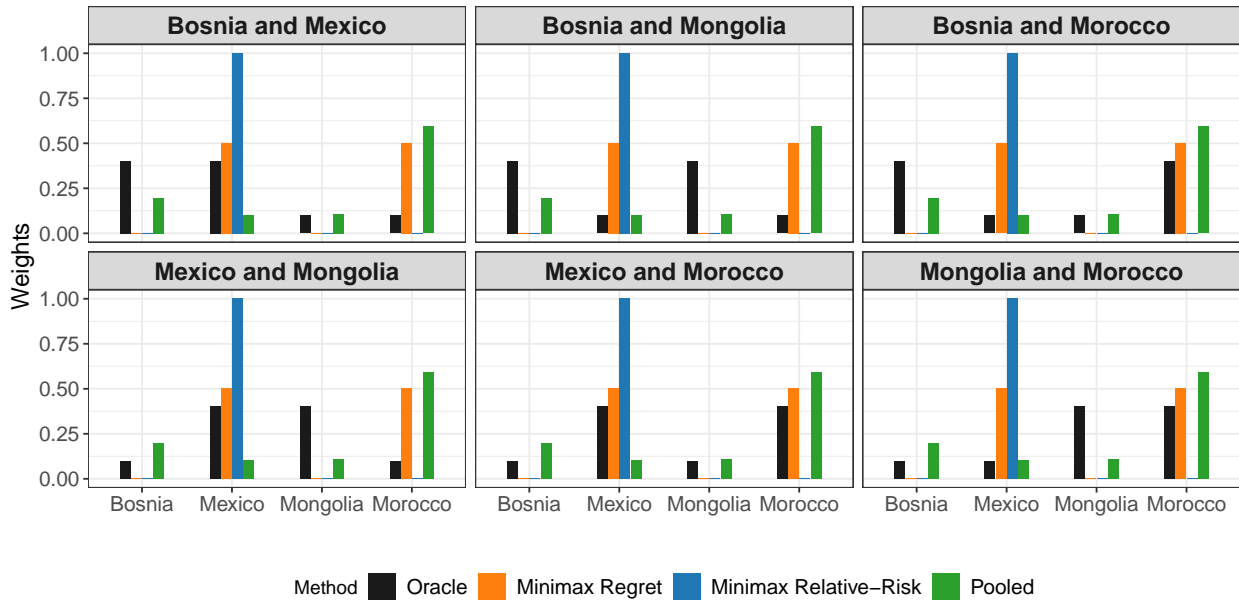


Figure D.5: Visualization of the weights estimated under each approach for (a) Scenario 3 and (b) Scenario 4. For the pooled approach, the estimated weights remain fixed and match the proportions implied by the source distributions. In other words, the pooled distribution is unable to adapt to the target population, even when the target distribution is very different from the source distributions. The weights for the minimax relative-risk approach consistently assigns a weight of 1 to Mongolia, and as such, considers a very conservative, worst-case scenario. The minimax regret approach assigns a weight of 0.5 to Mongolia, and 0.5 to Morocco.